Benchmarking noisy label detection methods

Henrique Pickler^a, Jorge K. S. Kamassury^a, Danilo Silva^a

^a Universidade Federal de Santa Catarina, R. Eng. Agronômico Andrei Cristian Ferreira, Florianópolis, 88040-900, Santa Catarina, Brazil

Abstract

Label noise is a common problem in real-world datasets, affecting both model training and validation. Clean data are essential for achieving strong performance and ensuring reliable evaluation. While various techniques have been proposed to detect noisy labels, there is no clear consensus on optimal approaches. We perform a comprehensive benchmark of detection methods by decomposing them into three fundamental components: label agreement function, aggregation method, and information gathering approach (in-sample vs out-of-sample). This decomposition can be applied to many existing detection methods, and enables systematic comparison across diverse approaches. To fairly compare methods, we propose a unified benchmark task, detecting a fraction of training samples equal to the dataset's noise rate. We also introduce a novel metric: the false negative rate at this fixed operating point. Our evaluation spans vision and tabular datasets under both synthetic and real-world noise conditions. We identify that in-sample information gathering using average probability aggregation combined with the logit margin as the label agreement function achieves the best results across most scenarios. Our findings provide practical guidance for designing new detection methods and selecting techniques for specific applications.

Keywords: Noisy label detection, Noisy labels, Dataset cleaning, Data quality, Benchmark, Neural networks

1. Introduction

Most supervised learning methods assume a perfectly labeled dataset. However, training data often contain incorrectly labeled instances. Even large, standard benchmark datasets, such as CIFAR, ImageNet, and MS-COCO, are known to have noisy labels [1, 2]. Label noise can originate from various sources, including human error, inherent data ambiguity, and automated labeling systems [3].

During training, label noise can significantly degrade model performance [3], as models tend to memorize incorrect labels [4]. To address this challenge, various methods have been proposed in the literature, including modifications to model architectures, the development of robust regularization techniques, and the design of noise-robust loss functions [5]. One interesting strategy is to identify noisy samples and leverage this information for training. For instance, removing these identified noisy samples can be advantageous even under imperfect detection [6, 7, 1], as their detrimental effect often outweighs the benefits of having more data. Another approach is to avoid the labels of identified noisy samples by using semi-supervised techniques [8, 9, 10], or self-supervised techniques [11], mitigating the negative effect of label noise while maintaining some of the benefits of having a larger dataset. A third approach involves (manually or automatically) relabeling these samples in order to have a cleaner dataset [12], enabling further training without using specific methods for noisy labels.

Moreover, the presence of label noise in a validation or test dataset can lead to misleading evaluations. If the noise is biased, model assessments based on such data may inherit and reflect that bias. In this context, label noise detection can be used to alleviate this issue, by identifying and helping correct mislabeled samples in the validation or test set.

While it is common to apply filtering (removing samples), semi-supervised learning (treating identified noisy samples as unlabeled), or relabeling (either automatically or manually) to achieve robust training

and evaluation, an important observation is that the detection stage is a distinct step that enables these relabeling strategies. As such, improving the criteria used for detection can enhance the overall effectiveness of these methods.

Be it noise in the training, validation or test set, detecting noisy samples is an important task to enable working with noisy datasets. Despite its importance in both robust training and robust evaluation, the detection task itself often receives limited attention as the focus tends to be on robust training outcomes, where the classification performance is generally the main metric observed [1, 9, 13, 6, 14, 15, 12]. While some methods briefly compare their proposed detection methods with others [6, 15, 14], they lack strong baselines, often rely on multiple metrics to evaluate methods on different operating points, or do not use the appropriate detection procedure associated with the methods being compared.

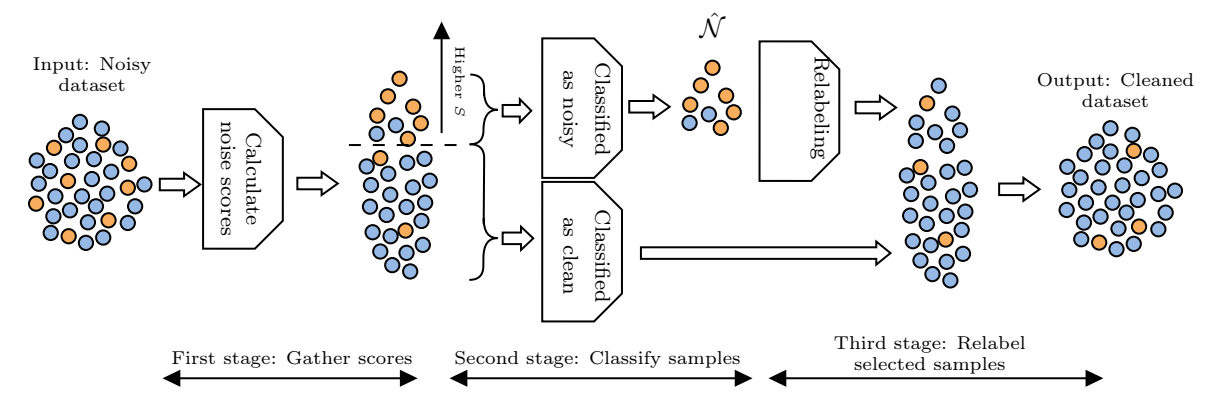


Figure 1: Illustration of the dataset cleaning process: Starting from a noisy dataset, scores are calculated to identify potentially mislabeled samples. Samples are detected as noisy or clean based on a threshold, with noisy samples relabeled to produce a cleaned dataset for downstream tasks.

Our primary contribution is to fill this gap by performing a comprehensive benchmark for comparing noisy label detection methods. The methods operate in a label-free setting, that is, no indication on which labels are wrong is provided.

Figure 1 shows the dataset cleaning process. While detection can be paired with various schemes to treat detected noisy samples (involving sample removal, label removal or label correction), we assume perfect relabeling in order to remove confounding factors and isolate detection performance. This lets us introduce a novel metric which is evaluated by detecting a fixed fraction of samples, ensuring a fair comparison between methods.

We decompose detection methods into two key components: label agreement function and aggregation technique. This allows us to systematically explore and propose seven new methods. One of the proposed methods frequently outperforms or matches the state of the art in most settings. We also explore in-sample and out-of-sample strategies such as Confident Learning. Our experiments show that in-sample methods tend to outperform out-of-sample ones.

- A comprehensive benchmark for noisy label detection: We introduce a unified evaluation framework where noise detection is performed without knowledge of which labels are corrupted and evaluated as a binary classification task.
- A modular analysis of detection methods: We decompose methods into label agreement functions and aggregation techniques, enabling the systematic creation of seven new detection methods and a clear comparison between in-sample and out-of-sample strategies.
- New insights and state-of-the-art performance: We find that aggregating prediction probabilities consistently outperforms loss-based aggregation, with one of our proposed methods frequently surpassing existing approaches.

2. Learning with Noisy Labels

Although this work focuses on detecting noisy labels, many detection methods are developed in the context of robust training and are often integrated into such approaches. Given this connection, we first formalize the problem of learning with label noise.

Consider the K-class classification task, where the feature space is denoted by \mathcal{X} , and the label space by $\mathcal{Y} \subseteq \{1, \ldots, K\}$. Let $\mathcal{D} = \{(x_i, y_i)\}_{i=1}^N$ be a set of examples, where the pairs $(x_i, y_i) \in \mathcal{X} \times \mathcal{Y}$ are random variables drawn from an unknown joint distribution P. In the classical supervised learning setting, the objective is to learn a function $f: \mathcal{X} \to \mathcal{Y}$, parameterized by Θ , that correctly reproduces the mapping of the feature space \mathcal{X} to the label space \mathcal{Y} given by P. For that, usually, an optimization of the parameters Θ is performed to minimize the empirical risk

$$\mathcal{R}_{\mathcal{D}}(f) = \frac{1}{|\mathcal{D}|} \sum_{i=1}^{|\mathcal{D}|} \ell(f(x_i; \Theta), y_i)$$
 (1)

where ℓ is an appropriate loss function.

In the context of label noise learning, however, we observe the set $\tilde{\mathcal{D}} = \{(x_i, \tilde{y}_i)\}_{i=1}^N$, where the labels \tilde{y}_i are drawn from a conditional distribution $P(\tilde{y}|x,y)$, referred to as the noise transition distribution. This means that the risk being minimized is actually

$$\mathcal{R}_{\tilde{\mathcal{D}}}(f) = \frac{1}{|\tilde{\mathcal{D}}|} \sum_{i=1}^{|\tilde{\mathcal{D}}|} \ell(f(x_i; \Theta), \tilde{y}_i). \tag{2}$$

The objective, then, is to learn a good model despite only having access to the noisy empirical risk. This can be a hard task, and multiple different methods have been proposed to train robust models in these conditions.

3. Detecting label noise

While much of the literature on learning with label noise focuses on training robust models in the presence of corrupted labels, a complementary and increasingly relevant line of work aims to identify which samples are likely mislabeled. The ability to detect noisy labels can enable more effective training strategies, such as sample selection, relabeling, semi-supervised or self-supervised robust training methods. In this work, we focus on the detection problem, which underpins the success of many noise-robust training methods.

3.1. Problem statement

To formalize the detection task, recall the definitions from subsection 2. We assume that the observed dataset $\tilde{\mathcal{D}}$, which is the dataset we intend to perform detection on, can be partitioned into two disjoint subsets: a clean set $\mathcal{C} = \{(x_i, \tilde{y}_i) : \tilde{y}_i = y_i, i \in \{1, \dots, N\}\}$ and a noisy set $\mathcal{N} = \tilde{\mathcal{D}} \setminus \mathcal{C}$. We define the detection labels as the vector that indicates whether a sample belongs to \mathcal{N} or not. This indication, however, is unknown in practice, and our goal is to infer it. That is, a detection method is a function that predicts whether a given sample belongs to \mathcal{N} , represented by

$$f_{\text{det}}: \mathcal{X} \times \mathcal{Y} \mapsto \{0, 1\},$$
 (3)

where $f_{\text{det}}(x_i, \tilde{y}_i) = 1$ indicates that the sample i is detected as noisy.

Most successful detection methods train models on the underlying classification task, then analyze training dynamics or model outputs to identify potentially mislabeled samples. This approach requires that training be performed on a dataset that includes the samples on which detection will be applied. Moreover, since better classification performance typically leads to improved detection accuracy, optimizing training hyperparameters becomes crucial. A noisy validation set drawn from the same distribution as $\tilde{\mathcal{D}}$ can facilitate this optimization process.

The detection process commonly involves calculating a noise score $S: \mathcal{X} \times \mathcal{Y} \to \mathbb{R}$ for each sample-label pair, quantifying the likelihood of mislabeling. This score is then thresholded to produce binary classifications, where the threshold can be tuned to balance sensitivity and specificity. While detection methods often include additional parameters beyond the threshold that substantially impact performance, tuning these parameters presents a significant challenge given the assumption of no access to ground-truth detection labels.

Finally, we focus on methods that perform detection based on model logits acquired during training, as these can be directly integrated into standard training pipelines without additional architectural considerations. Specifically, given the logits $z_i^{[t]} \in \mathbb{R}^K$ for sample i gathered during epoch t (more precisely, during the corresponding step where sample i is processed within epoch t), the detection function is

$$f_{\text{det}}(\{z_i^{[t]}\}_{t=1}^E, \hat{y}_i) \in \{0, 1\}.$$
 (4)

where E is the total number of training epochs.

While there are approaches that rely on other approaches—for instance, [16] uses a cross-validation strategy to measure the impact of individual samples on held-out accuracy, and [17] proposes a feature-clustering method that bypasses model training altogether—these fall outside the scope of our study. We also exclude embedding-based approaches such as the Centrality and Consistency method [13], which employs a two-stage strategy based on learned representations. Although these methods are conceptually interesting, they introduce significant additional design and implementation considerations. For instance, embedding-based techniques require isolating and manipulating intermediate model components (e.g., freezing the feature extractor, retraining classifiers), which diverges from the simpler and more unified setting of prediction-based methods that can be directly applied during standard model training.

3.2. In-sample detection methods

In-sample detection methods are widely used to identify noisy labels. These methods generally extract information for each sample during the training process, exploiting the early learning phenomenon [18]. Most methods follow a similar approach and can be described by two steps: (i) gathering label agreement measures for every sample using a label agreement function L (frequently taken to be a loss function, e.g., cross-entropy in O2U-net), and (ii) aggregating these measures to produce a final noise score for each sample. We start by describing commonly used aggregation methods.

Last epoch: Uses the loss of each sample at the final epoch of training, providing a snapshot of how well the model's prediction aligns with the assigned label. This approach is equivalent to the criterion used in Co-teaching and DivideMix:

$$S(x_i, \tilde{y}_i) = L(z_i^{[E]}, \tilde{y}_i). \tag{5}$$

where $z_i^{[E]}$ are the final epoch logits.

Mean agreements: Averages the agreement measures of a sample over the entire training. Expressed by

$$S(x_i, \tilde{y}_i) = \frac{1}{E} \sum_{t=1}^{E} \left(L(z_i^{[t]}, \tilde{y}) \right).$$
 (6)

CTRL: Identifies noisy samples by clustering loss trajectories across temporal windows [14]. The method preprocesses loss trajectories applying clipping and smoothing, divides training into windows, then clusters samples by loss patterns within each class and window using K-means. Samples in high-loss clusters are flagged across windows, and a voting mechanism produces final noise scores.

Temporal ensemble: Instead of analyzing loss trajectories, this approach aggregates model probabilities over training epochs, inspired by Snapshot Ensembles [19] and briefly explored in Dataset Cartography [20]. That is,

$$\bar{\hat{p}}_i = \frac{1}{E} \sum_{t=1}^E \operatorname{softmax}(z_i^{[t]}), \tag{7}$$

where softmax is the softmax function. We generalize the original method by converting the probabilities back to logits using the logarithmic function, that is

$$\bar{z}_i = \log \bar{\hat{p}}_i + C \tag{8}$$

where the logarithmic function is applied component-wise. Setting C=0, we can define the noise scoring function as

$$S_i = L(\bar{z}_i, \tilde{y}_i). \tag{9}$$

Stochastic weight averaging (SWA): Aggregates model parameters collected over training epochs. After training for E epochs, we average the model parameters from all epochs:

$$\bar{z}_i = f\left(x_i; \frac{1}{E} \sum_{t=1}^E \Theta^{[t]}\right) \tag{10}$$

where $\Theta^{[t]}$ are the parameters of the model at the end of epoch t and the final scoring is given by Equation 9.

Importantly, none of the aggregation techniques introduced above depend on a specific function L. In fact, L may be any measure that quantifies the agreement between a model's prediction and the sample's assigned label. For clarity, we will refer to L as the label agreement function, and in the remainder of this subsection we describe the specific label agreement functions employed in this work.

Cross Entropy (CE) loss: The standard classification loss, equivalent to negative log-probability of the assigned class. Since the logarithmic function is monotonic, it produces an equivalent ranking as using the negative of the probability of the assigned class.

Jensen-Shannon (JS) divergence: A symmetric version of the Kullback-Leibler (KL) divergence that measures distributional similarity

$$L_{JSD}(\hat{p}_i, \tilde{y}_i) = \frac{1}{2} \mathcal{D}\left(\hat{p}_i || \frac{\tilde{e}_i + \hat{p}_i}{2}\right) + \frac{1}{2} \mathcal{D}\left(\tilde{e}_i || \frac{\tilde{e}_i + \hat{p}_i}{2}\right), \tag{11}$$

where $\tilde{e}_{i,k} = \mathbb{1}(\tilde{y}_i = k)$ is the k-th entry of the one-hot encoded noisy label for the i-th sample and \mathcal{D} is the Kullback-Leibler divergence. For one-hot labels, JS divergence maintains a monotonic, non-linear, relationship with the cross-entropy loss.

Logit Margin (LM): Measures the difference between the assigned class logit and the highest other class logit. It was proposed in [15] for label noise detection, where it is used together with the mean aggregation to produce a noise score, referred to as the AUM (Area Under the Margin) score. We use the negative formulation to align with other measures:

$$L_{LM}(z_i, \tilde{y}_i) = \max_{k \neq \tilde{y}_i} z_{i,k} - z_{i,\tilde{y}_i}, \tag{12}$$

Higher values indicate disagreement with the assigned label. This is equivalent to using the negative log-ratio between the assigned class probability and the highest other class probability.

Many detection methods can be seen as combinations of one of these aggregation methods and one of the agreement functions. For example, the detection method used by Co-teaching and DivideMix can be thought of being the Last aggregation combined with the CE loss. O2U-net is the combination of the Mean aggregation with the CE loss and the method used in UniCon can be thought of being the Last combined with the JS divergence, which, in our case, is equivalent to using the CE loss. Dataset cartography originally uses the mean probabilities of the assigned class over the epochs. We know, however, that this is equivalent to using the Mean Probabilities combined with the CE loss or JS divergence. The original CTRL method uses the CE loss, however, it can be used with other measures. In fact, by separating the methods into these two steps, we allow the combination of different aggregation methods and label agreement functions.

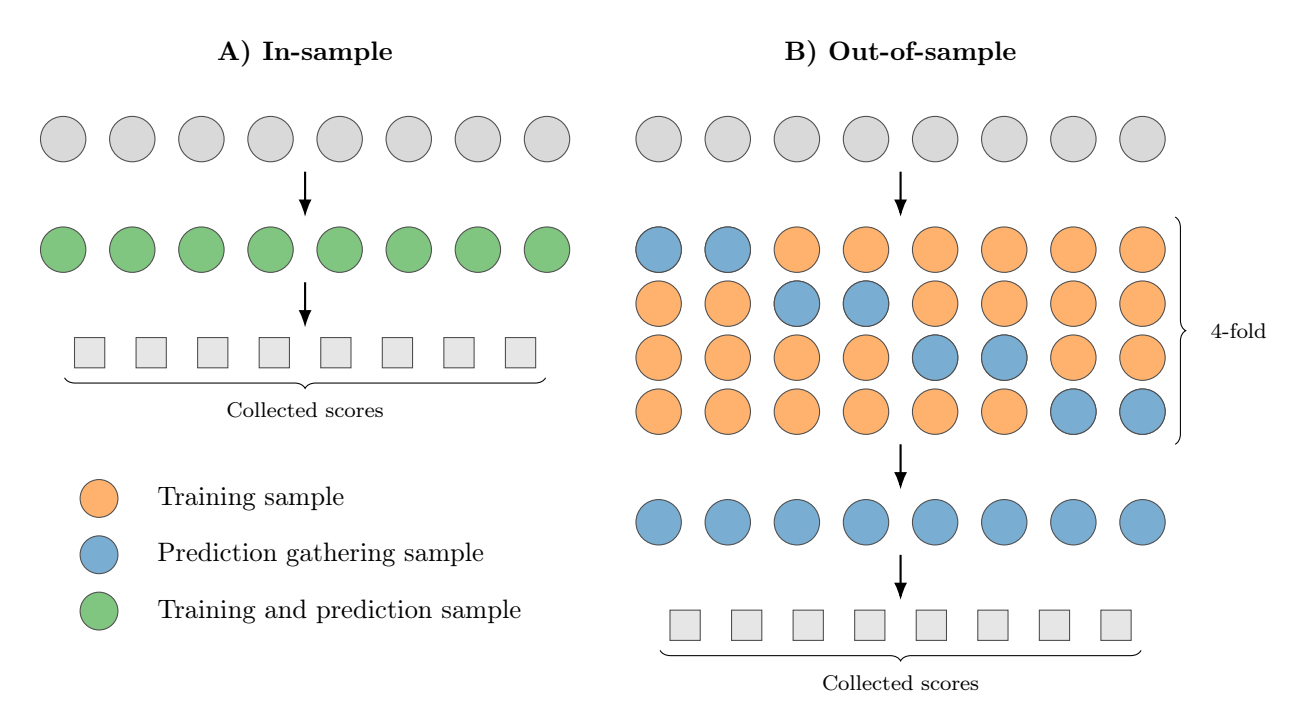


Figure 2: Data gathering representation for in-sample and out-of-sample methods. Blue circles indicate samples for which predictions are stored, red circles indicate samples used only for training and purple samples indicate samples in which both training and gathering of predictions are made.

3.3. Out-of-sample detection methods

Out-of-sample methods use cross-validation to obtain predictions from models that have not seen specific samples during training, avoiding memorization effects.

Iterative Noisy Cross-Validation (INCV): [21] iteratively partitions the dataset, training models on clean samples to identify additional clean samples in held-out portions. At each iteration, samples where the model agrees with the label are marked as clean, while a fraction of high-loss samples are flagged as noisy.

Confident Learning: [1] constructs a "confident joint matrix" from K-fold predictions, counting samples where predicted probabilities exceed class-specific thresholds. This matrix estimates the joint distribution of true and observed labels. Three detection variants are proposed: (1) $C_{\rm confusion}$ (CC) - flagging samples where model predictions disagree with the label, (2) Prune by Class (PBC) - selecting lowest-confidence samples per class based on estimated noise rates, and (3) Prune by Noise Rate (PBNR) - selecting samples by prediction margin for each class pair.

We focus on Confident Learning, as INCV's iterative approach introduces additional complexity and hyperparameters that complicate direct comparisons. Furthermore, we note that most other detection methods could also be applied iteratively, thus, we leave this exploration for future work.

3.4. Related works

Throughout this section and the introduction, we have reviewed a variety of label noise detection methods. Although several papers include empirical comparisons [6, 15, 14], these evaluations are typically narrow in scope. They often compare against only one or two baselines, focusing on validating a new algorithm rather than establishing broad, reproducible rankings. Furthermore, many existing benchmarks exhibit methodological limitations, such as limited hyperparameter tuning of baselines, inconsistent adherence to each method's intended detection protocol, and the use of metrics without a clearly defined operating point. These issues hinder fair comparison and highlight the need for a more systematic benchmark, which motivates our work.

To the best of our knowledge, the work by [12] is the only prior study that systematically evaluates multiple detection methods in a unified framework. The authors investigate strategies for allocating a fixed labeling budget—a relevant problem when relabeling is imperfect and multiple annotations may be required to obtain a confidently correct label. Under a limited budget, this creates a trade-off between acquiring new samples and correcting existing (possibly) mislabeled ones. The authors propose a resource allocation strategy and evaluate its impact on the performance of the resulting classification model. This allocation is guided by different detection methods, where they evaluate the following methods: AUM, Large Loss—using the loss of the last epoch—and dataset cartography.

Our experimental setup shares similarities with theirs, particularly in the use of detection methods to guide relabeling. However, some differences exist. First, their work focuses on data acquisition, needing to balance between gathering new data and fixing gathered noisy data. Our problem concerns only one of the steps in their experimental setup: noise detection. To focus specifically on this task, we assume all samples have an initial (possibly noisy) label and fix the fraction of samples to be cleaned in each setting. This removes the trade-off between label correction and data acquisition, enabling a more direct comparison between detection methods. We also assume perfect relabeling, that is, every detected sample gets assigned its correct label instead of going through a (possibly) wrong new labeling process. With this, we focus only on errors made by detection, removing the confusion between detection and relabeling errors.

4. Methods

In this section, we present the primary metric used to compare detection methods, describe the procedure for optimizing these methods, and provide details on training, hyperparameter tuning, datasets, and other key aspects that ensure reproducibility.

4.1. Evaluating detection methods

Similar to binary classification, the task of detecting noisy labels involves identifying which samples belong to one of two classes, namely, the noisy set \mathcal{N} or the clean set \mathcal{C} . Intending to compare different methods, we measure the remaining noise after performing a cleaning pass. In more detail, we assume that every sample detected as noisy, composing the set $\hat{\mathcal{N}}$, will be correctly relabeled by a specialist. This means that the number of noisy samples originally is

$$|\mathcal{N}| = |\mathcal{N} \cap \hat{\mathcal{N}}| + |\mathcal{N} \cap (\tilde{\mathcal{D}} \setminus \hat{\mathcal{N}})| = t_p + f_n, \tag{13}$$

where $t_p = |\mathcal{N} \cap \hat{\mathcal{N}}|$ indicates the number of true positives (correctly identified noisy samples) and $f_n = |\mathcal{N} \cap (\tilde{\mathcal{D}} \setminus \hat{\mathcal{N}})|$ the number of false negatives (noisy samples incorrectly identified as clean). We can then define the noise rate as

$$\eta = \frac{|\mathcal{N}|}{N} = \frac{f_n + t_p}{N}.\tag{14}$$

After cleaning, all true positive samples will be corrected, while the false negatives will remain unchanged. Thus, the number of residual noisy samples simply becomes f_n . Then, the residual noise rate is given by $\eta_{res} = \frac{f_n}{N}$. Finally, we define the normalized residual noise rate as

$$\rho_{\eta} = \frac{\eta_{res}}{\eta} = \frac{f_n}{f_n + t_p} = \text{FNR}$$
(15)

where FNR stands for false negative rate. This metric describes the proportion of noise, with respect to the original noise fraction, that persists after cleaning the samples detected as noisy. Since it coincides exactly with the FNR, this is how we will refer to it.

Note that increasing the sensitivity of a method will always either maintain or decrease the FNR, since we assume ideal cleaning. Increasing the sensitivity, however, also increases the number of samples to be analyzed, thus increasing the necessary effort for cleaning. This means that there is a trade-off between the amount of work and the amount of noise left. Better detection methods improve this trade-off by minimizing

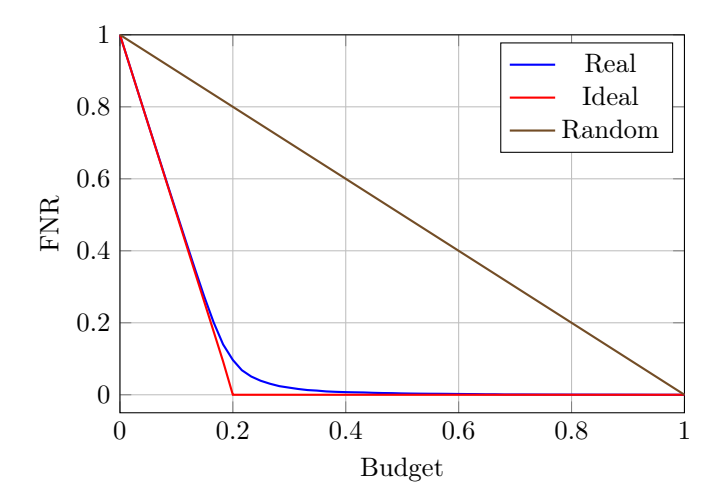


Figure 3: Example of the budget x FNR curve for an ideal, random and a real method in a setting with $\eta = 0.2$.

the effort necessary to achieve a given FNR. Likewise, a better detection method would result in a smaller FNR for the same amount of effort.

We analyze this trade-off by parameterizing the detection task by a budget $b \in [0, 1]$, which represents the fraction of positive predictions. In more detail, let $S \in \mathbb{R}^N$ be the score produced by a detection method for each sample, and $\pi: \{1, \ldots, N\} \mapsto \{1, \ldots, N\}$ be a permutation of the indices that would produce a sorted version of S, with ties broken in an arbitrary but deterministic order. Then we can define the predicted noisy set

$$\hat{\mathcal{N}} = \{ (x_{\pi(i)}, \tilde{y}_{\pi(i)}) : i \in \{1, \cdots, \lceil bN \rceil \} \}.$$

Since tied values are ordered arbitrarily, the selection among samples with equal scores is effectively random, and the detection outcome within this tied region is equivalent to that of a random detector. Naturally, this also works for methods that produce highly discretized scoring. For methods that produce a direct prediction, we encode S as follows: 1 for samples predicted as noisy and 0 for samples predicted as clean.

For an ideal detection method, the remaining noise fraction for a given budget is expressed as:

$$FNR_{ideal}(b) = \begin{cases} 1 - \frac{b}{\eta} & \text{if } b < \eta \\ 0 & \text{if } b \ge \eta \end{cases}$$
 (16)

That is, a piece-wise linear function going from (0,1) to $(\eta,0)$ and then (1,0). Notably, a random detector is represented by a line going from (0,1) to (1,0). Both detectors are represented in Figure 3 together with a real detection method.

An interesting metric to consider is the value of $FNR(\eta)$, that is, the remaining noise after cleaning a fraction of samples equal to the noise rate. The ideal model has $FNR_{ideal}(\eta) = 0$ for any noise rate, thus, this measure would indicate how much relative noise is left due to the imperfection of the detection method used. Evaluating at η also takes into account the natural necessity of increasing the number of samples to investigate in noisier cases. We choose this metric to evaluate detection methods because it summarizes the performance of a method in one single number at a relevant operating point.

To fairly compare between the techniques for detecting noisy labels, we propose a unified benchmarking protocol focusing on noisy label detection. In this setting, each method performs a measurement gathering phase which may include multiple training rounds, allowing for the accumulation of signals to identify potential noise patterns. This approach serves as a basis for all methods to operate within a consistent framework, facilitating an objective comparison.

4.2. Detection methods

In total we explore 15 different detection methods. These methods are combinations of the aggregation techniques and label agreement functions reviewed in the previous section.

The in-sample methods are the combinations of:

- 1. Aggregation techniques: Last, Mean, Mean Probabilities, CTRL and SWA
- 2. Label agreement functions: Cross-Entropy Loss, Jensen-Shannon Divergence and Logit Margin

Table 1 shows the combinations explored for in-sample methods and their relation to existing methods. Additionally, we include three out-of-sample methods from the confident learning framework [1]: $C_{\text{confusion}}$, Prune By Class, and Prune By Noise Rate.

		Aggregatio	n		
Measure	Last	Mean Probability	SWA	Mean	CTRL
Cross-Entropy	Co-teaching			O2U-net	CTRL
Jensen-Shannon	DivideMix Unicon	Dataset Cartography	0	0	0
Logit Margin	0	0	0	AUM	0

Table 1: Relation between aggregation-measure combinations and existing in-sample detection methods. Blank cells with o represent combinations evaluated in this work but not previously explored. Cross-Entropy and Jensen-Shannon measures yield identical results under 'Last', 'Mean Probability' and 'SWA' aggregations.

4.3. Datasets and Settings

We evaluate all methods on multiple computer vision and tabular datasets, incorporating both synthetic and real noise. We provide the contingency matrices for each setting on Appendix A. In the following subsubsections, we detail each dataset, the pre-processing procedures, the label noise generation methods (when applicable), and the neural network architectures used in our experiments.

While many noise types exist in the literature, we focus on symmetric and pairflip noise as they represent complementary extremes of noise sparsity while being easily described solely by noise rate. Symmetric noise affects all classes uniformly (dense), whereas pairflip noise has sparse noise transition. To complement these synthetic noise types, we also evaluate on real-world noise, which captures the complex patterns found in actual datasets.

For all tabular datasets, we follow the pre-processing methodology described in [14], with one exception for the Cardiotocography dataset. Instead of using all 33 features as in the original work, we retain only the 21 features explicitly recommended in the dataset documentation, as some of the excluded features are not suitable for inference.

4.3.1. Model Architectures

For CIFAR datasets, we use the 9-layer Convolutional Neural Network (CNN) architecture proposed in [7]. For Clothing1M, we employ ResNet-18 (Residual Network), while for Food-101N, we use ResNet-34 (Residual Network). For all tabular datasets, we implement a Multilayer Perceptron (MLP) architecture optimized for each specific setting, following [14].

4.3.2. Classification Hyperparameter Optimization

For each dataset and noise level, we perform a manual optimization of the learning rate, learning rate scheduler, batch size, and weight decay by observing the 10-epoch rolling mean accuracy on a held-out noisy validation set. To determine the optimal number of training epochs, we first train the model for a large number of epochs while monitoring validation performance. We then identify the epoch that maximizes the validation metric and retrain the model from scratch for that specific number of epochs.

Dataset	#	Original features	Transformed features	Classes	Train/Test Split
CIFAR-10	60K	32×32	32×32	10	50K / 10K
CIFAR-100	60K	32×32	32×32	100	$50\mathrm{K}\ /\ 10\mathrm{K}$
CIFAR-10N	60K	32×32	32×32	10	$50\mathrm{K}~/~10\mathrm{K}$
Clothing1M	1M+	Varied (mostly 256×256) ¹	224×224	14	$1\mathrm{M}{+}24\mathrm{K}~/~10\mathrm{K}$
Food-101N	310K	Varied $_2$ (320–512 px typical)	128×128	101	$285\mathrm{K}~/~25\mathrm{K}$
Cardiotocography	2126	21	21	3	$1700 \ / \ 426$
Credit Fraud	$285\mathrm{K}^3$	30	30	2	1107 / 369
Human Activity Detection	10299	561	30	6	$7352\ /\ 2947$
Letter Recognition	20K	16	16	26	$15000 \ / \ 5000$
Mushroom	7864	22	67	2	$5898 \ / \ 1966$
Satellite	6435	36	36	6	4435 / 2000
Sensorless Drive	59K	48	48	11	$43882 \ / \ 14627$

¹ Images range from 60×84 to 461×1399 ; Around 80% are 256×256 .

Table 2: Dataset statistics

We tailor the optimization strategy to each dataset type. For datasets with synthetic noise, we extensively optimize without noise first (both training and validation sets are clean) and then fine-tune the hyperparameters with noisy labels (both training and validation sets are noisy). For Food-101N and Clothing1M datasets, we optimize with noisy labels only. For tabular datasets, we also search for an MLP architecture following [14] while also optimizing the learning rate in {0.0001, 0.001, 0.001} and weight decay in {0,0.001}.

All detection methods use these optimized hyperparameters when training models to collect detection signals. For out-of-sample methods, which require cross-validation, we perform the K-fold procedure within the training set only. All final hyperparameter settings are given in Appendix B, and the accuracies achieved on the test set are given in Appendix C.

4.4. Detection Hyperparameter Optimization

Outside of the choice of threshold, noisy label detection methods are generally considered hyperparameter-free and independent of the training procedure. It is generally assumed that optimizing the classification task improves the detection performance indirectly. Interestingly, prior work [6] has demonstrated that modifying training dynamics, such as cyclically varying the learning rate, can significantly enhance detection performance even though classification performance may remain the same.

Optimizing training specifically for detection is beyond the scope of this paper. Instead, we follow a simpler approach and optimize only the aggregation window used by certain methods. These methods (e.g., Mean - CE, Mean Probas - LM and Last - CE) rely on aggregating an agreement measure (such as the cross-entropy or logit margin) across multiple training epochs. The choice of which interval of epochs to aggregate over, the aggregation window, may significantly affect detection performance.

Our approach follows a simple yet effective two-step procedure:

- 1. Training: We fully train the model for twice as long as the original training epochs, saving the output logits for all samples at each epoch.
- 2. Post-hoc Optimization: Using the saved predictions, we search for the best aggregation window by selecting intervals of epochs (start and end) without the need for retraining.

² Images range from 80×70 to 1511×3874 ; most common are 426×320 , 320×426 , 320×320 , and 512×512 .

³ Subsampled to balance classes with a ratio of 1:2 of positive to negative examples.

Dataset	Training Transforms	Test Transforms
	Vision Datasets	
CIFAR-10 CIFAR-100 CIFAR-10N	4px padding Random crop (32×32) Horizontal flip (50%) Normalization	Normalization
Clothing1M	Resize (256×256) Random crop (224×224) Horizontal flip (50%) Normalization	Resize Center crop (224×224) Normalization
Food-101N	Random resize crop with scale $[0.08, 1.0] \rightarrow 128 \times 128$ Horizontal flip (50%) Normalization	Resize (min edge = 128) Center crop (128×128) Normalization
	Tabular Datasets*	
Cardiotocography	Clip out Standard	
Credit Fraud	Clip outliers (Q PCA (n_compo Clip PC fe Standard :	onents= 0.9) atures ²
Letter	Clip outliers (Q Standard :	
Mushroom	Drop constan Category cons One-hot er Standard	solidation ³ acoding
Satellite	Clip outliers (Q Standard	
Sensorless Drive	Clip outliers (Q Standard:	

^{*}Same transforms used for training and testing. $^1\mathrm{ALTV}\colon Q_{2\%}\text{-}Q_{95\%},$ others: $Q_2\%\text{-}Q_{98}\%$ $^2PC_0\colon Q_1\%\text{-}Q_{99}\%,$ others: $Q_{25}\%\text{-}Q_{75}\%$ $^3\mathrm{Low-frequency}$ categories grouped as 'other'

Table 3: Overview of the transforms used in each dataset

To find the optimal window, we search over 50 equally spaced epochs for the starting and final aggregation epochs, leading to a total of at most 1250 aggregation windows. Figure 4 shows the processes and acquired data necessary for optimization.

In the case of the CTRL method, which employs clustering over multiple time windows, we optimize its own hyperparameters post-hoc via grid search. We explore combinations of the number of time windows $\{2,4,8\}$, the number of clusters per window $\{2,4,8\}$, and the number of selected clusters $\{1,3,7\}$.

For selecting these hyperparameters, we propose leveraging a detection tuning set, that is, a small subset of samples with indication of whether the original label is noisy or not. In this experiment, we reserve 10% of the training dataset as tuning data for the detection task (note that this detection tuning data remains part of the training data). To evaluate the amount of annotation required, we experiment with different proportions of labeled data (10%, 5% and 1%). We evaluate methods on the remaining 90% of training data, in contrast to the benchmark evaluation, where methods are assessed on the entire training set. Figure 5 shows the splits used in this work.

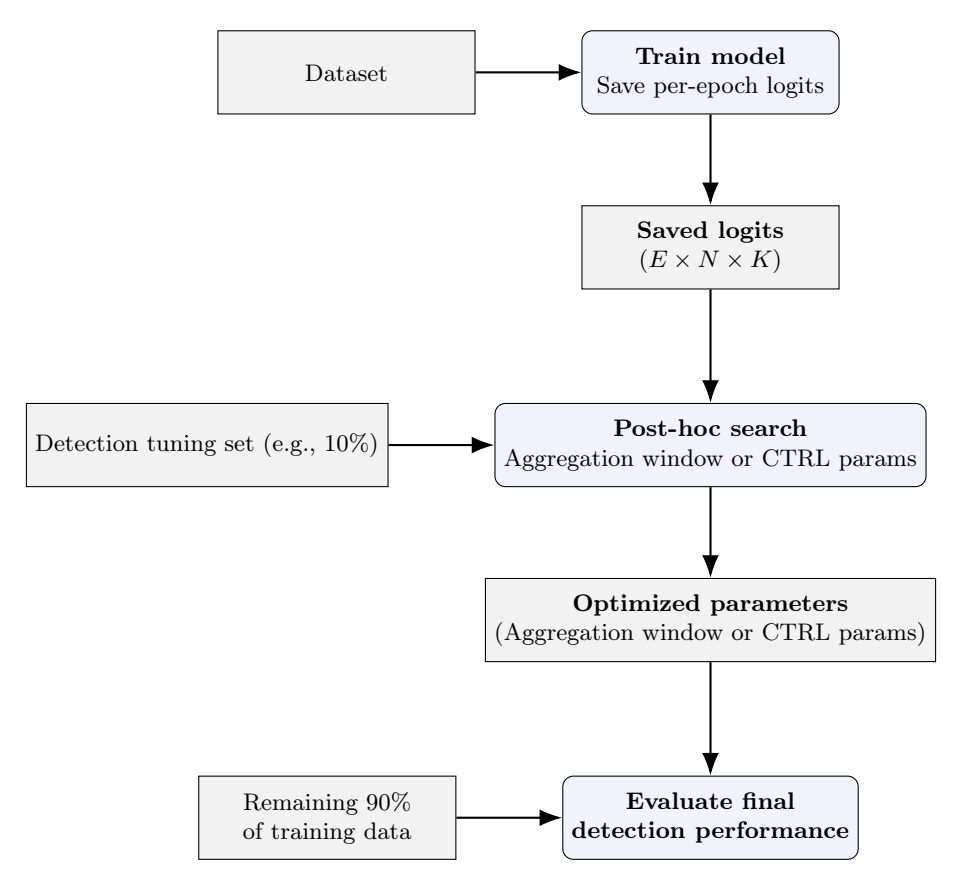


Figure 4: Workflow for training and post-hoc detection optimization. The model is trained once, and the logits for each sample are saved across epochs. A small detection tuning set is used to select the best aggregation window or CTRL hyperparameters, which are then evaluated in the remaining dataset.

5. Results and Discussion

5.1. Main Findings

Mean Probabilities with Logit Margin (Mean Prob - LM) emerges as the most consistently effective approach for noisy label detection across diverse noise scenarios, representing a novel contribution that has not been previously explored. This combination achieves robust performance across 17 different scenarios spanning synthetic and real-world datasets.

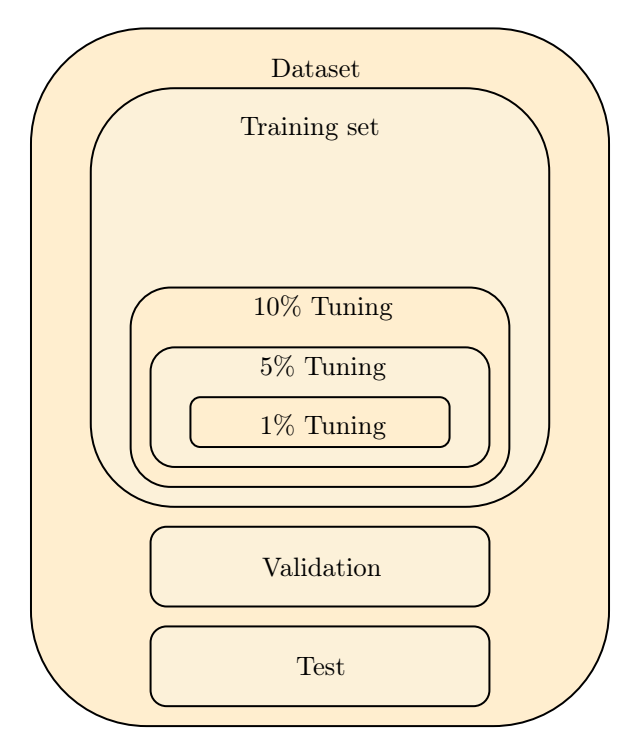


Figure 5: The dataset splits used in this work. The dataset is divided into the usual train-validation-test splits for classification. One additional type of split is made for detection, represented by the three tuning splits used for tuning the detection methods.

5.2. Noisy Label Detection Benchmark

Tables 4-6 present false negative rates (FNR) at a budget equal to the noise rate across datasets with synthetic noise (vision and tabular) and real-world noise (vision only).

The choice of label alignment function significantly impacts performance across different noise types. For instance, Logit Margin excels in pairflip scenarios, where its ability to capture decision boundary proximity makes it sensitive to this type of noise pattern. This advantage also extends to real-world datasets like CIFAR-10N and Clothing1M, where noise tends to be sparse and structured. In symmetric noise scenarios, while Logit Margin still generally outperforms Jensen-Shannon, the performance gap is considerably smaller than in pairflip settings. Jensen-Shannon also demonstrates strong performance on Food-101N, but without knowledge of the noise pattern, the underlying cause remains unclear. These findings suggest that aligning the scoring metric with the underlying noise structure can yield substantial performance improvements, with the choice being most critical in specific noise contexts like pairflip scenarios.

Equally important is the aggregation strategy employed. Mean and Mean Probabilities consistently outperform Last aggregation, with Mean Probabilities demonstrating particular strength in challenging scenarios. These improvements show an asymmetric pattern: when Mean Probabilities outperforms other methods, it delivers substantial gains of 5-10% improvement in FNR, but when it underperforms relative to other methods, the losses are minimal at typically less than 2% difference.

Surprisingly, more sophisticated methods fail to justify their complexity. Despite theoretical advantages, neither SWA nor CTRL provided consistent improvements. CTRL's performance volatility, showing competitive results on CIFAR-10 pairflip but worst-case performance on CIFAR-10 symmetric 20%, challenges the assumption that explicitly modeling training dynamics enhances detection. Similarly, Confident Learning's out-of-sample approach, designed to avoid memorization effects, consistently underperformed simpler in-sample methods using temporal ensembles.

Tables 7 and 8 confirm these findings persist even when accounting for discretization effects, with Mean Prob - LM maintaining significant advantages over reference methods at their respective operating points

Model			9-Laye	er CNN		
Dataset		CIFAR-10			CIFAR-100	
Noise type	Pairflip	Symr	netric	Pairflip	Symr	netric
Noise rate	20.00%	20.00%	50.00%	20.00%	20.00%	50.00%
Last - CE/JS	13.31 ± 0.38	9.13 ± 0.15	8.53 ± 0.07	49.07 ± 0.37	12.33 ± 0.09	9.59 ± 0.11
Last - LM	11.65 ± 0.45	9.55 ± 0.23	8.60 ± 0.15	29.36 ± 0.48	15.78 ± 0.14	10.82 ± 0.08
Mean - CE	15.47 ± 0.11	7.50 ± 0.13	5.99 ± 0.07	47.48 ± 0.41	9.73 ± 0.07	8.61 ± 0.01
Mean - JS	10.24 ± 0.03	7.58 ± 0.11	5.97 ± 0.06	43.94 ± 0.32	9.74 ± 0.12	8.53 ± 0.05
Mean - LM	8.40 ± 0.08	7.16 ± 0.09	5.61 ± 0.04	22.27 ± 0.41	8.88 ± 0.08	8.17 ± 0.06
Mean Prob - CE/JS	8.19 ± 0.08	7.62 ± 0.10	5.93 ± 0.07	41.66 ± 0.47	9.75 ± 0.10	8.51 ± 0.07
Mean Prob - LM	6.16 ± 0.06	7.25 ± 0.05	5.69 ± 0.01	17.83 ± 0.35	9.41 ± 0.09	8.87 ± 0.03
CTRL - CE	9.46 ± 0.39	20.59 ± 0.30	8.35 ± 0.17	47.79 ± 0.34	45.14 ± 0.21	19.64 ± 0.17
CTRL - JS	16.58 ± 0.49	36.32 ± 0.28	16.99 ± 0.31	59.90 ± 0.59	61.94 ± 0.30	33.27 ± 0.36
CTRL - LM	28.20 ± 0.60	43.45 ± 0.20	13.33 ± 0.27	53.82 ± 0.33	50.64 ± 0.23	11.62 ± 0.33
CL - CC	33.67 ± 0.23	32.09 ± 0.32	17.49 ± 0.04	57.83 ± 0.47	61.02 ± 0.18	32.88 ± 0.11
CL - PBC	23.01 ± 0.59	12.50 ± 0.49	10.04 ± 0.04	46.57 ± 0.15	29.57 ± 0.23	18.22 ± 0.16
CL - PBNR	22.64 ± 0.58	14.61 ± 0.39	10.54 ± 0.14	35.62 ± 0.46	38.56 ± 0.19	25.80 ± 0.16
SWA - CE/JS	19.52 ± 0.18	11.94 ± 0.18	8.85 ± 0.04	55.66 ± 0.46	16.12 ± 0.13	11.98 ± 0.11
SWA - LM	14.27 ± 0.29	12.88 ± 0.16	9.10 ± 0.08	36.98 ± 0.29	17.95 ± 0.37	13.58 ± 0.02

Table 4: FNR (%) measured for a budget equal to the noise rate on CIFAR-10 and CIFAR-100. Best results are shown in bold.

Model	9-Laye	r CNN	ResNet-18	ResNet-34
Dataset	CIFA	R-10N	Clothing1M	Food-101N
Noise type	Aggregate	Worse	Real	Real
Noise rate	9.01%	40.21%	38.26%	18.51%
Last - CE/JS	33.45 ± 0.31	15.95 ± 0.13	32.02 ± 0.53	43.92 ± 0.15
Last - LM	33.26 ± 0.19	15.04 ± 0.10	30.19 ± 0.49	46.28 ± 0.24
Mean - CE	26.67 ± 0.12	17.23 ± 0.15	32.04 ± 0.12	35.93 ± 0.03
Mean - JS	25.87 ± 0.12	16.15 ± 0.16	31.62 ± 0.12	33.61 ± 0.13
Mean - LM	24.03 ± 0.24	13.16 ± 0.09	28.91 ± 0.11	37.60 ± 0.02
Mean Prob - CE/JS	25.37 ± 0.06	15.37 ± 0.13	31.37 ± 0.19	33.00 ± 0.07
Mean Prob - LM	23.29 ± 0.20	$12.61\pm{\scriptstyle 0.01}$	28.05 ± 0.32	35.12 ± 0.09
CTRL - CE	38.50 ± 0.08	13.33 ± 0.08	34.35 ± 0.05	49.99 ± 0.18
CTRL - JS	54.82 ± 0.39	18.75 ± 0.23	33.23 ± 0.43	60.91 ± 0.49
CTRL - LM	69.36 ± 1.13	19.64 ± 0.24	49.12 ± 0.18	67.35 ± 0.02
CL - CC	49.79 ± 0.18	18.92 ± 0.27	33.32 ± 0.22	57.63 ± 0.22
CL - PBC	38.35 ± 0.56	16.71 ± 0.08	45.21 ± 0.42	42.62 ± 0.32
CL - PBNR	42.51 ± 0.23	20.60 ± 0.19	41.77 ± 0.22	58.10 ± 0.57
SWA - CE/JS	33.67 ± 0.21	18.20 ± 0.10	32.17 ± 0.10	68.41 ± 0.11
SWA - LM	33.28 ± 0.06	16.16 ± 0.11	30.17 ± 0.18	68.17 ± 0.19

Table 5: FNR (%) measured for a budget equal to the noise rate on the real-world noise datasets CIFAR-10N, Clothing1M and Food-101N. Best results are shown in bold.

Model				MLP			
Dataset	Cardioto- cography	Credit Fraud	Human Activity	Letter	Mushroom	Satellite	Sensorless Drive
Noise type	Symmetric	Symmetric	Symmetric	Symmetric	Symmetric	Symmetric	Symmetric
Noise rate	20.00%	20.00%	20.00%	20.00%	20.00%	20.00%	20.00%
Last - CE/JS	36.31 ± 10.36	15.08 ± 5.36	31.57 ± 1.57	9.40 ± 0.20	2.53 ± 0.27	11.05 ± 0.35	0.74 ± 0.05
Last - LM	37.13 ± 10.96	15.08 ± 5.36	29.61 ± 1.49	8.42 ± 0.16	2.53 ± 0.27	11.43 ± 0.35	0.69 ± 0.03
Mean - CE	30.17 ± 4.62	11.92 ± 0.94	5.69 ± 0.41	3.48 ± 0.21	0.26 ± 0.00	10.43 ± 0.13	0.65 ± 0.02
Mean - JS	29.99 ± 5.01	11.92 ± 0.94	7.09 ± 0.63	4.14 ± 0.22	0.29 ± 0.05	10.43 ± 0.13	0.66 ± 0.01
Mean - LM	30.62 ± 5.41	11.92 ± 0.94	7.97 ± 0.44	3.03 ± 0.08	0.29 ± 0.05	10.82 ± 0.13	0.59 ± 0.01
Mean Prob - CE/JS	30.17 ± 5.09	11.92 ± 0.94	8.96 ± 0.49	4.44 ± 0.28	0.26 ± 0.00	10.47 ± 0.18	0.65 ± 0.02
Mean Prob - LM	30.62 ± 5.64	11.92 ± 0.94	8.49 ± 0.37	3.66 ± 0.06	0.26 ± 0.00	10.93 ± 0.07	0.59 ± 0.00
CTRL - CE	40.02 ± 11.84	31.52 ± 3.46	18.93 ± 0.81	6.99 ± 0.20	6.68 ± 0.59	30.25 ± 1.51	0.63 ± 0.06
CTRL - JS	38.84 ± 14.24	27.15 ± 6.70	26.45 ± 0.79	17.08 ± 0.72	3.77 ± 0.42	40.11 ± 0.41	37.57 ± 0.14
CTRL - LM	53.84 ± 10.51	43.59 ± 2.65	56.17 ± 0.21	44.37 ± 0.84	51.60 ± 5.38	47.15 ± 0.66	47.58 ± 0.85
CL - CC	48.15 ± 3.50	44.19 ± 0.69	46.83 ± 7.06	41.30 ± 0.70	2.12 ± 0.58	35.22 ± 1.11	24.87 ± 0.99
CL - PBC	42.19 ± 4.41	34.24 ± 0.94	29.09 ± 4.85	22.24 ± 1.00	1.44 ± 0.28	15.36 ± 1.10	12.51 ± 1.19
CL - PBNR	42.28 ± 4.26	34.24 ± 0.94	29.23 ± 5.09	23.54 ± 0.91	1.44 ± 0.28	15.40 ± 1.10	13.37 ± 1.34
SWA - CE/JS	28.46 ± 3.30	12.22 ± 0.90	5.85 ± 0.97	3.53 ± 0.26	0.21 ± 0.05	11.28 ± 0.58	0.80 ± 0.01
SWA - LM	29.27 ± 4.26	12.22 ± 0.90	6.48 ± 0.92	3.11 ± 0.12	0.21 ± 0.05	11.78 ± 0.42	0.71 ± 0.05

Table 6: FNR (%) measured for a budget equal to the noise rate on tabular datasets. Best results are shown in bold.

across both synthetic vision noise scenarios and real-world noise datasets. Note that these results are measured for a budget equal to the operating point of the reference method; since operating points with lower budgets lead to higher FNRs, the absolute values should not be solely interpreted as method performance. Furthermore, operating points differ across each group of rows and columns, making cross-comparison not meaningful.

Model			9-Laye	r CNN		
Dataset		CIFAR-10			CIFAR-100	
Noise type	Pairflip	Symr	netric	Pairflip	Symr	netric
Noise rate	20.00%	20.00%	50.00%	20.00%	20.00%	50.00%
CTRL - CE Mean Prob - LM	4.917 ± 0.188 2.574 ± 0.047	1.920 ± 0.160 2.089 ± 0.035	4.183 ± 0.134 3.815 ± 0.140	5.518 ± 1.473 1.284 ± 0.237	$\begin{array}{c} 1.233 \pm 0.057 \\ 1.253 \pm 0.058 \end{array}$	3.003 ± 0.040 2.531 \pm 0.095
CL - PBC Mean Prob - LM	13.67 ± 0.09 1.887 ± 0.058	5.068 ± 0.167 3.285 ± 0.138	5.477 ± 0.605 2.972 ± 0.276	31.36 ± 0.87 3.130 ± 0.400	4.401 ± 0.589 1.462 ± 0.102	6.453 ± 0.217 2.606 \pm 0.061
CL - PBNR Mean Prob - LM	7.279 ± 0.158 1.963 ± 0.065	8.845 ± 0.133 3.690 ± 0.101	9.269 ± 0.224 4.754 ± 0.098	15.02 ± 0.38 3.245 ± 0.109	26.41 ± 0.34 2.656 \pm 0.077	28.68 ± 0.95 13.81 ± 1.20

Table 7: FNR (%) at the operating point of the reference method on CIFAR-10 and CIFAR-100 with synthetic noise.

5.3. Impact of hyperparameter optimization on detection performance

Tables 9, 10, and 11 present detection performance after hyperparameter tuning for each method (see Appendix D for hyperparameter values). The results demonstrate that hyperparameter optimization has minimal impact on overall performance: across datasets, noise types, and noise rates, tuning rarely alters the relative ranking of methods and produces only marginal improvements in most experimental conditions. The qualitative conclusions drawn from untuned (default) configurations remain valid after optimization. The few instances of non-negligible improvements are concentrated in Last and CTRL aggregation methods. For Last-CE, we observe that optimization primarily corrects subpar performance in specific datasets by adjusting the final training epoch, suggesting these improvements address artifacts from the early-stopping procedure (see Figure 6). For CTRL-CE, while optimization can yield significant improvements, this likely

Model	9-Layer	CNN	ResNet-18	ResNet-34
Dataset	CIFAI	R-10N	$\overline{ ext{Clothing1M}}$	Food-101N
Noise type	Aggregate	Worse	Real	Real
Noise rate	9.01%	40.21%	38.26%	18.51%
CTRL - CE Mean Prob - LM	8.258 ± 0.465 6.911 ± 0.243	14.30 ± 1.12 13.97 ± 1.55	39.02 ± 3.68 34.37 ± 4.77	$16.21 \pm 0.98 \\ 15.52 \pm 0.77$
CL - PBC Mean Prob - LM	39.26 ± 0.41 32.59 ± 0.36	17.34 ± 0.18 15.36 ± 0.14	60.25 ± 0.22 58.43 ± 0.21	41.29 ± 0.20 34.41 ± 0.07
CL - PBNR Mean Prob - LM	43.26 ± 0.18 32.04 ± 0.54	22.10 ± 0.22 18.56 \pm 0.08	53.04 ± 0.20 51.96 ± 0.55	58.22 ± 0.78 35.54 ± 0.64

Table 8: FNR (%) at the operating point of the reference method on real-world noise datasets.

reflects the discretization issues identified in the previous section. Additionally, since other methods were partially optimized by selecting the training epochs in our baseline experiments, CTRL may show more dramatic optimization effects. Notably, even after tuning, CTRL-CE remains inferior to simpler methods across nearly all scenarios.

6. Conclusion

In this work, we presented a benchmark for label noise detection, systematically evaluating a range of methods across multiple datasets and noise scenarios. Among our key findings, we show that the Mean Probabilities aggregation is particularly effective under non-symmetric noise distributions. The Logit Margin also performs well in this context, and by combining both, we arrive at a new detection method, Mean Probabilities - LM. This combination consistently delivers robust performance across a variety of settings. However, we also observe that for datasets with a large number of classes and symmetric noise, using Mean Probabilities - CE/JS can be a suitable alternative.

Our results further reveal that in-sample detection methods tend to outperform out-of-sample ones, suggesting that memorization does not impact the detection performance significantly. Interestingly, methods previously thought to leverage training dynamics may, in practice, be benefiting from temporal ensembling instead. This is supported by the relatively poor performance of CTRL, which aims to exploit temporal information, compared to the ensemble-based Mean Probabilities approach. Notably, this performance gap persists even after accounting for discretization effects and hyperparameter optimization. Overall, this simpler interpretation of previously proposed methods may be helpful in advancing research in this area.

While ensemble methods show clear advantages, our experiments indicate that using SWA yields inferior performance compared to other ensemble strategies. One potential explanation is that aggregating weights from early training epochs—when models are less reliable—can degrade performance more than aggregating output probabilities. This insight suggests that tuning the aggregation window for SWA could lead to improved results, although such post-hoc adjustments would significantly increase storage requirements.

We also explored the sensitivity of detection methods to hyperparameter tuning. In particular, we found that Mean Probabilities - LM demonstrates low sensitivity to hyperparameter changes. This is a valuable property, as hyperparameter optimization often requires relabeling a significant fraction of samples to evaluate detection performance. Given the minimal performance gains observed, such optimization efforts may not be justified, especially when resources could be more efficiently allocated by using the unoptimized method directly.

Although the post-hoc optimization performed appears to offer limited benefit, optimizing the training process itself for detection may unlock further improvements in noise detection. For instance, prior work by [6] demonstrates that using a cyclic learning rate schedule can enhance detection performance. However,

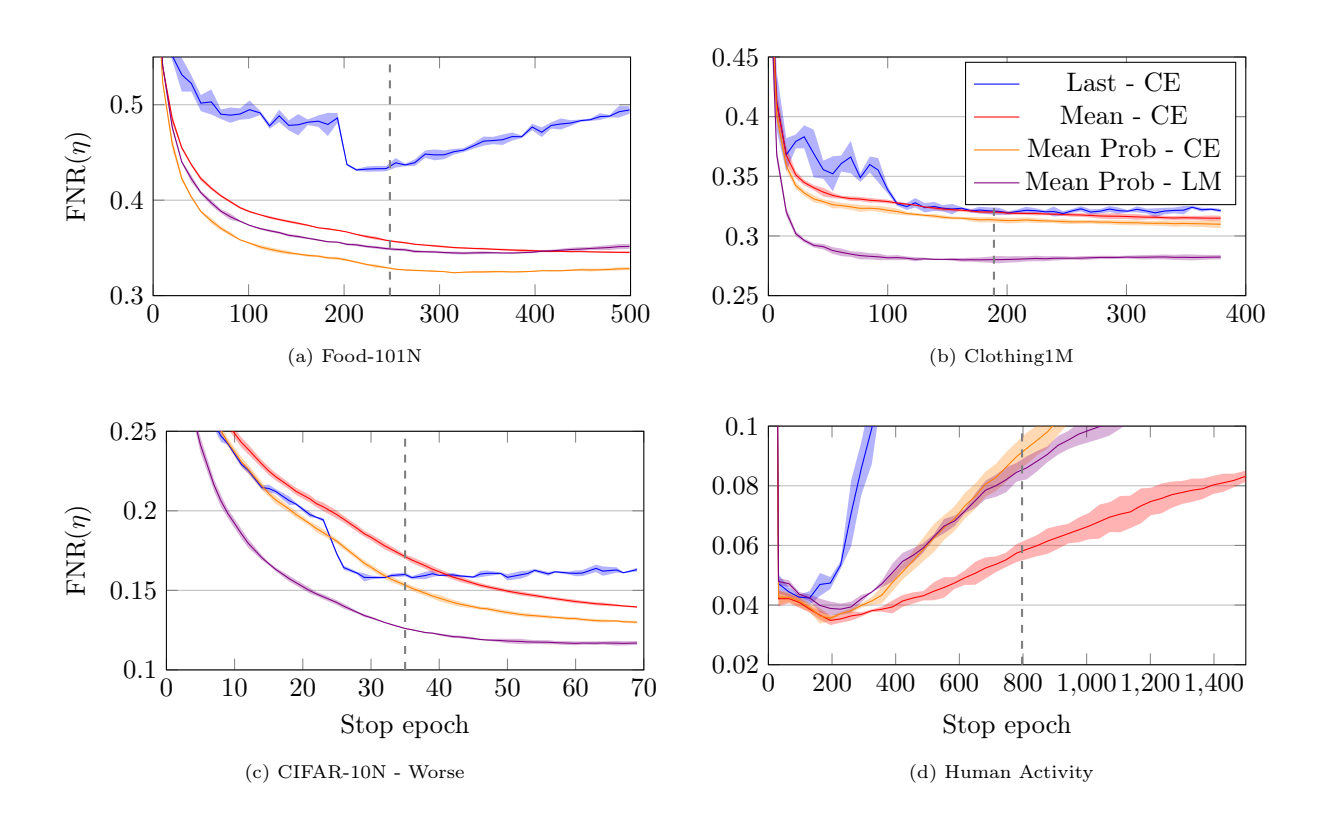


Figure 6: FNR at noise rate varying the final epoch of the aggregating window on four datasets, measured on the remaining 90% of data. The vertical black dotted line indicates the original amount of training epochs.

	Model			9-Laye	er CNN		
	Dataset		CIFAR-10			CIFAR-100	
	Noise type	Pairflip	Symn	netric	Pairflip	Symn	netric
	Noise rate	20.00%	20.00%	50.00%	20.00%	20.00%	50.00%
Fraction	Method						
0%	Last - CE/JS Mean - CE Mean Prob - LM CTRL - CE	13.35 ± 0.39 15.45 ± 0.18 6.19 ± 0.07 9.42 ± 0.37	9.14 ± 0.16 7.54 ± 0.12 7.23 ± 0.04 20.62 ± 0.46	8.48 ± 0.11 5.97 ± 0.07 5.67 ± 0.02 8.35 ± 0.16	49.09 ± 0.41 47.54 ± 0.43 17.91 ± 0.28 48.32 ± 0.49	12.26 ± 0.12 9.71 ± 0.07 9.44 ± 0.09 45.05 ± 0.32	9.56 ± 0.09 8.62 ± 0.02 8.83 ± 0.01 19.83 ± 0.28
1%	Last - CE/JS Mean - CE Mean Prob - LM CTRL - CE	13.29 ± 0.17 7.71 ± 0.25 $\mathbf{5.24 \pm 0.03}$ 8.22 ± 0.19	8.92 ± 0.02 6.60 ± 0.10 6.02 ± 0.10 6.29 ± 0.08	8.15 ± 0.02 5.97 ± 0.07 5.25 ± 0.09 6.20 ± 0.11	47.80 ± 0.81 41.17 ± 0.53 16.79 ± 0.05 35.50 ± 0.43	12.66 ± 0.10 9.62 ± 0.06 9.64 ± 0.10 13.71 ± 0.21	9.50 ± 0.23 7.65 ± 0.08 8.77 ± 0.07 8.64 ± 0.12
5%	Last - CE/JS Mean - CE Mean Prob - LM CTRL - CE	13.40 ± 0.34 8.07 ± 0.30 5.12 ± 0.03 8.22 ± 0.19	8.92 ± 0.02 6.25 ± 0.02 6.13 ± 0.09 6.29 ± 0.08	8.50 ± 0.07 5.82 ± 0.10 5.26 ± 0.11 5.56 ± 0.12	47.80 ± 0.81 39.63 ± 0.28 16.52 ± 0.14 35.50 ± 0.43	12.55 ± 0.11 9.37 ± 0.08 9.30 ± 0.08 9.62 ± 0.32	9.42 ± 0.03 7.77 ± 0.06 8.16 ± 0.07 7.96 ± 0.12
10%	Last - CE/JS Mean - CE Mean Prob - LM CTRL - CE	13.40 ± 0.34 7.85 ± 0.18 5.19 ± 0.04 8.22 ± 0.19	9.21 ± 0.08 6.25 ± 0.02 6.10 ± 0.06 6.29 ± 0.08	8.32 ± 0.05 5.41 ± 0.05 5.23 ± 0.09 5.56 ± 0.12	47.80 ± 0.81 39.67 ± 0.32 16.60 ± 0.08 35.50 ± 0.43	12.66 ± 0.10 9.37 ± 0.15 9.34 ± 0.07 9.62 ± 0.32	9.42 ± 0.03 7.73 ± 0.03 8.18 ± 0.07 7.96 ± 0.12

Table 9: Results for optimization on vision datasets with synthetic noise across different held-out fractions for detection method tuning. Every method is evaluated on the remaining 90% of data. Values in bold indicate the best result for each fraction, while values in both bold and italic represent the best overall across all fractions.

optimizing training for detection presents significant challenges, such as the increased computational cost due to multiple training rounds. Moreover, data-efficient strategies need to be developed to allow optimization on small tuning sets without risking overfitting.

While we have explored vision and tabular datasets, a natural extension for this work is to consider other dataset domains and tasks such as text, audio, time series, and other classification tasks. We use a range of noise types from symmetric noise to real-world noise; however, other noise types may be challenging and reveal weaknesses and strengths of each method, such as asymmetric noise and instance noise. Exploring how different model architectures, such as transformer-based models, affect detection would be valuable as well. Incorporating different label noise learning techniques during the training phases for detection may also yield significant improvements.

Acknowledgements

This work was supported in part by the Brazilian National Council for Scientific and Technological Development (CNPq-Brazil) under Grants 304619/2022-1 and 402516/2024-9, and in part by Fundacao de Amparo à Pesquisa e Inovacao do Estado de Santa Catarina (FAPESC) under Grant 2024TR000090.

Appendix A. Contingency Tables

Figures A.7-A.9 provide the contingency matrices for each setting. We present them in a heatmap where, for easier visualization, the counts of the correct labels are not included in the color bar.

Since Food-101N only provides a value indicating if a sample is clean or noisy, it is not possible to compute a contingency matrix. We provide instead, the noise rate for each class on Figure A.10.

For the Clothing1M dataset we use only the subset of data in the training set that has both clean and noisy labels. We note that on Clothing1M the 4th class is plagued with much more noise than correct labels,

	Model	9-Layer	r CNN	ResNet-18	ResNet-34
	Dataset	CIFA	R10N	Clothing1M	Food-101N
	Noise type	Aggregate	Worse	Real	Real
	Noise rate	$\overline{9.01\%}$	$\phantom{00000000000000000000000000000000000$	$\phantom{00000000000000000000000000000000000$	$\phantom{00000000000000000000000000000000000$
Fraction	Method				
	Last - CE/JS	33.47 ± 0.46	16.00 ± 0.12	32.03 ± 0.52	43.83 ± 0.21
0%	Mean - CE	26.65 ± 0.15	17.12 ± 0.14	31.99 ± 0.15	35.76 ± 0.04
U70	Mean Prob - LM	23.24 ± 0.22	12.60 ± 0.03	28.03 ± 0.28	34.92 ± 0.16
	CTRL - CE	38.36 ± 0.38	13.30 ± 0.05	34.37 ± 0.27	49.85 ± 0.23
	Last - CE/JS	35.64 ± 0.29	16.17 ± 0.06	32.08 ± 0.18	43.17 ± 0.12
1%	Mean - CE	24.62 ± 0.04	12.77 ± 0.08	32.08 ± 0.18	34.46 ± 0.21
170	Mean Prob - LM	22.49 ± 0.33	12.08 ± 0.05	28.17 ± 0.15	34.72 ± 0.24
	CTRL - CE	43.31 ± 0.44	14.34 ± 0.04	32.78 ± 0.19	35.15 ± 0.10
	Last - CE/JS	30.89 ± 0.84	15.81 ± 0.05	31.94 ± 0.38	43.31 ± 0.28
5%	Mean - CE	25.18 ± 0.09	12.74 ± 0.10	31.38 ± 0.17	34.27 ± 0.19
370	Mean Prob - LM	22.23 ± 0.07	11.65 ± 0.11	28.13 ± 0.19	34.68 ± 0.08
	CTRL - CE	26.12 ± 0.35	14.34 ± 0.04	32.78 ± 0.19	35.15 ± 0.10
	Last - CE/JS	30.89 ± 0.84	16.02 ± 0.20	31.94 ± 0.38	43.31 ± 0.28
1007	Mean - CE	24.83 ± 0.28	12.76 ± 0.09	31.32 ± 0.21	34.35 ± 0.16
10%	Mean Prob - LM	22.53 ± 0.09	11.76 ± 0.11	28.27 ± 0.21	34.72 ± 0.24
	CTRL - CE	26.12 ± 0.35	14.34 ± 0.04	32.78 ± 0.19	35.40 ± 0.11

Table 10: Results for optimization on vision datasets with real noise across different held-out fractions for detection method tuning. Every method is evaluated on the remaining 90% of data. Values in bold indicate the best result for each fraction, while values in both bold and italic represent the best overall across all fractions.

	Model				MLP			
	Dataset	Cardioto- cography	Credit Fraud	Human Activity	Letter	Mushroom	Satellite	Sensorless Drive
	Noise type	Symmetric	Symmetric	Symmetric	Symmetric	Symmetric	Symmetric	Symmetric
	Noise rate	20.00%	20.00%	20.00%	20.00%	20.00%	20.00%	20.00%
Fraction	Method							
0%	Last - CE/JS Mean - CE Mean Prob - LM CTRL - CE	35.14 ± 10.09 29.02 ± 4.36 29.42 ± 5.04 40.66 ± 12.88	15.08 ± 4.38 11.89 ± 0.77 12.06 ± 1.01 32.50 ± 4.06	31.58 ± 1.75 5.82 ± 0.30 8.53 ± 0.39 19.56 ± 0.91	9.34 ± 0.22 3.34 ± 0.21 3.53 ± 0.06 6.87 ± 0.18	2.45 ± 0.29 0.23 ± 0.06 0.26 ± 0.06 6.63 ± 0.83	11.04 ± 0.34 10.31 ± 0.07 10.91 ± 0.13 30.34 ± 2.35	0.73 ± 0.05 0.65 ± 0.01 0.59 ± 0.01 0.66 ± 0.07
1%	Last - CE/JS Mean - CE Mean Prob - LM CTRL - CE	30.22 ± 2.85 31.33 ± 2.87 31.02 ± 3.13 37.35 ± 12.24	22.11 ± 2.51 15.75 ± 2.48 15.91 ± 2.77 13.90 ± 1.05	4.44 ± 0.15 4.21 ± 0.15 4.72 ± 0.11 9.00 ± 0.53	4.93 ± 0.18 3.17 ± 0.16 3.09 ± 0.09 4.50 ± 0.07	$\begin{array}{c} \textbf{2.42} \pm \textbf{0.20} \\ 5.00 \pm 0.26 \\ 5.20 \pm 0.35 \\ 3.86 \pm 0.32 \end{array}$	12.58 ± 0.46 13.39 ± 0.27 11.55 ± 0.22 $\boldsymbol{9.20} \pm 0.52$	$egin{array}{l} \textbf{0.89} & \pm \ \textbf{0.06} \\ 1.02 & \pm \ 0.03 \\ \textbf{0.88} & \pm \ \textbf{0.02} \\ 1.00 & \pm \ 0.01 \end{array}$
5%	Last - CE/JS Mean - CE Mean Prob - LM CTRL - CE	30.22 ± 2.85 28.61 ± 3.19 30.42 ± 3.39 42.07 ± 16.21	12.23 ± 1.05 11.89 ± 1.05 11.89 ± 1.05 14.74 ± 0.29	4.24 ± 0.23 3.49 ± 0.16 3.89 ± 0.23 5.52 ± 0.22	3.86 ± 0.20 3.67 ± 0.28 3.21 ± 0.22 4.00 ± 0.20	1.34 ± 0.15 1.47 ± 0.20 1.93 ± 0.11 3.86 ± 0.74	10.70 ± 0.32 10.70 ± 0.32 11.60 ± 0.20 9.20 ± 0.52	0.75 ± 0.12 0.68 ± 0.02 0.69 ± 0.03 0.95 ± 0.01
10%	Last - CE/JS Mean - CE Mean Prob - LM CTRL - CE	30.22 ± 2.85 29.82 ± 3.26 29.82 ± 3.65 38.55 ± 14.24	13.57 ± 1.01 11.73 ± 0.77 11.56 ± 0.87 14.74 ± 0.29	4.69 ± 0.39 4.16 ± 0.23 4.49 ± 0.28 5.92 ± 1.04	3.86 ± 0.20 3.33 ± 0.25 2.94 ± 0.18 4.00 ± 0.20	0.23 ± 0.20 0.46 ± 0.20 0.42 ± 0.23 3.86 ± 0.74	11.13 ± 0.27 11.13 ± 0.27 12.15 ± 0.32 9.20 ± 0.52	0.75 ± 0.12 0.68 ± 0.02 0.66 ± 0.01 0.89 ± 0.01

Table 11: Results for optimization on tabular datasets with synthetic noise across different held-out fractions for detection method tuning. Every method is evaluated on the remaining 90% of data. Values in bold indicate the best result for each fraction, while values in both bold and italic represent the best overall across all fractions.

with 149 correct labels and 1185 wrong labels. We have observed that in this class most detection methods fail, presenting random detection.

Appendix B. Hyperparameters

Table B.12 provides the hyperparameters used for training on each setting.

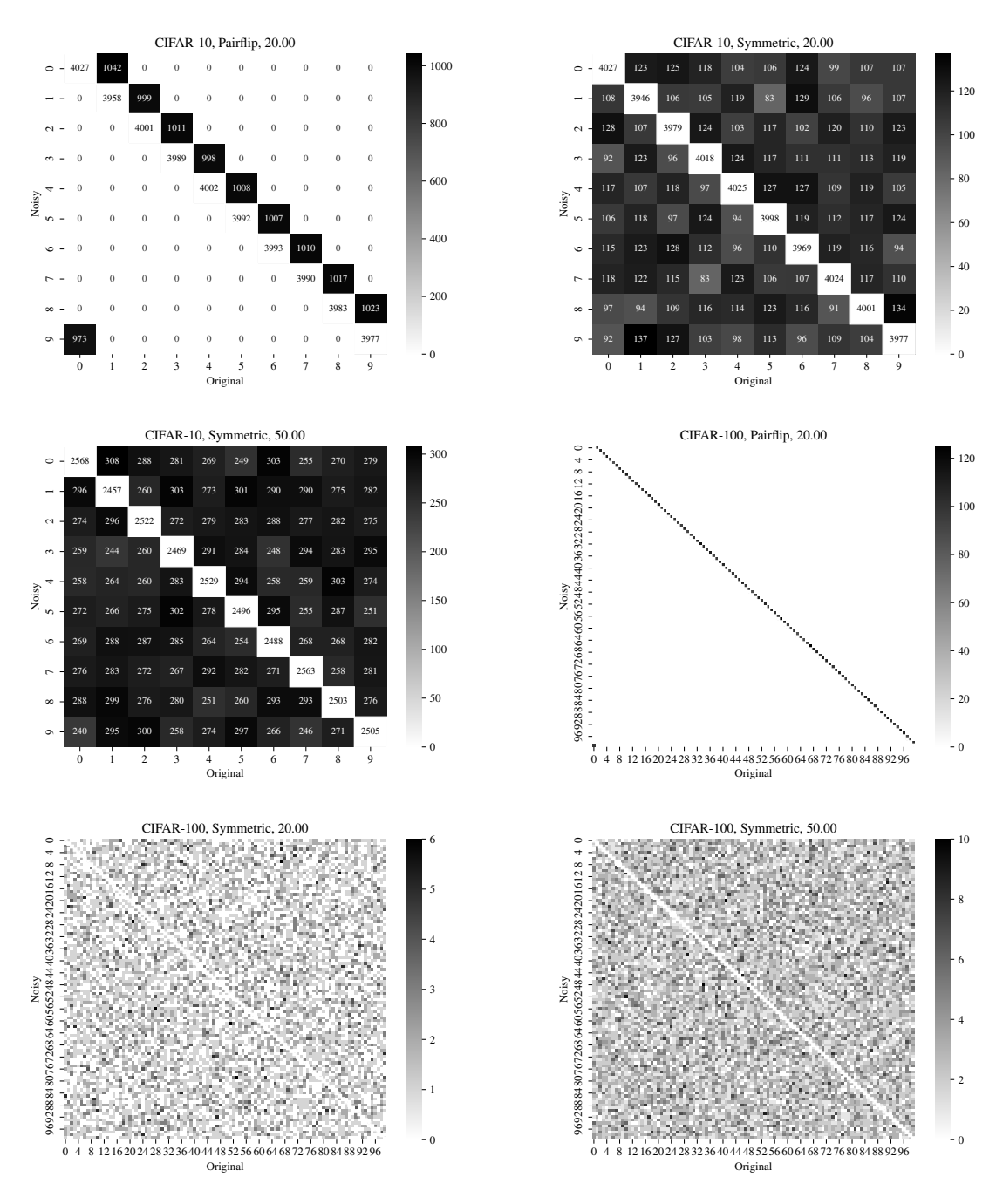


Figure A.7: Contingency tables for synthetic noise vision datasets.

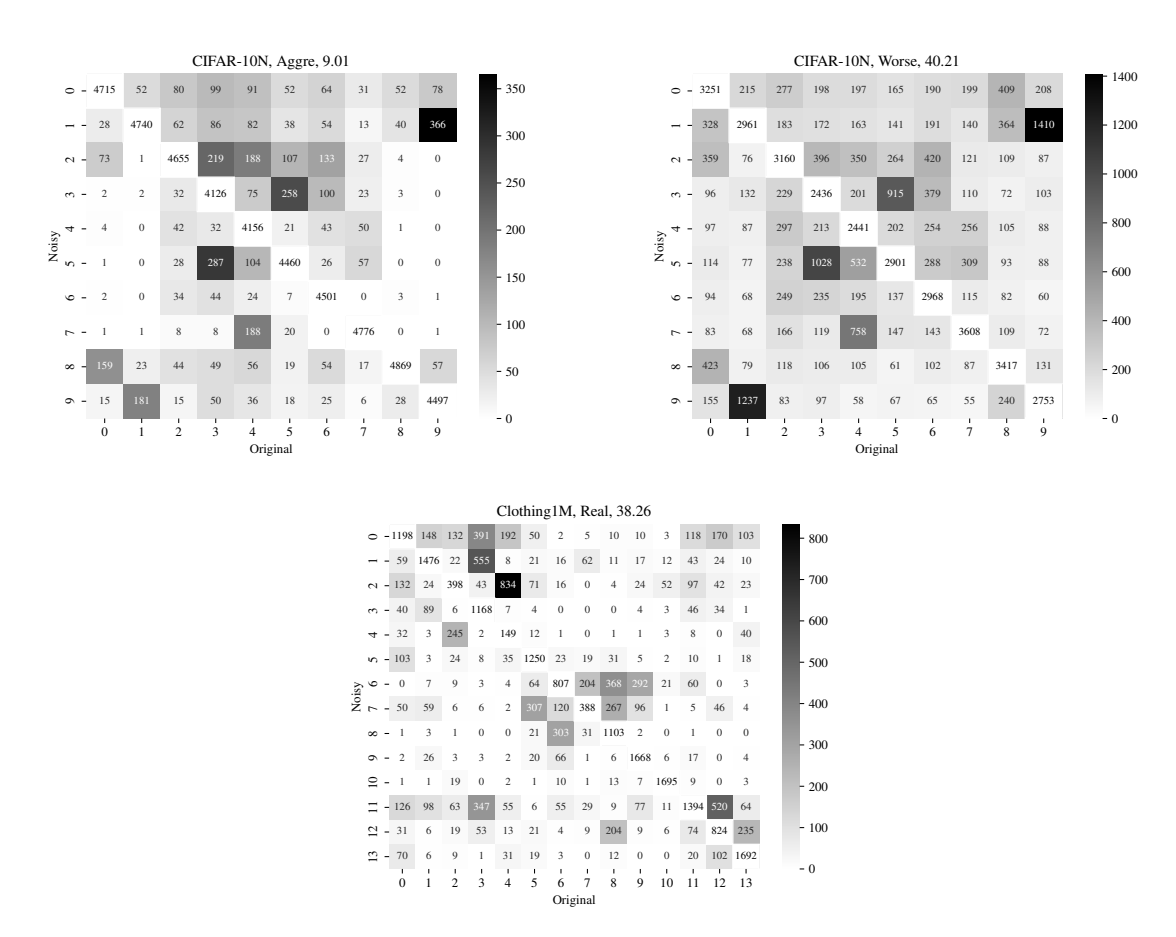


Figure A.8: Contingency tables for real noise vision datasets.

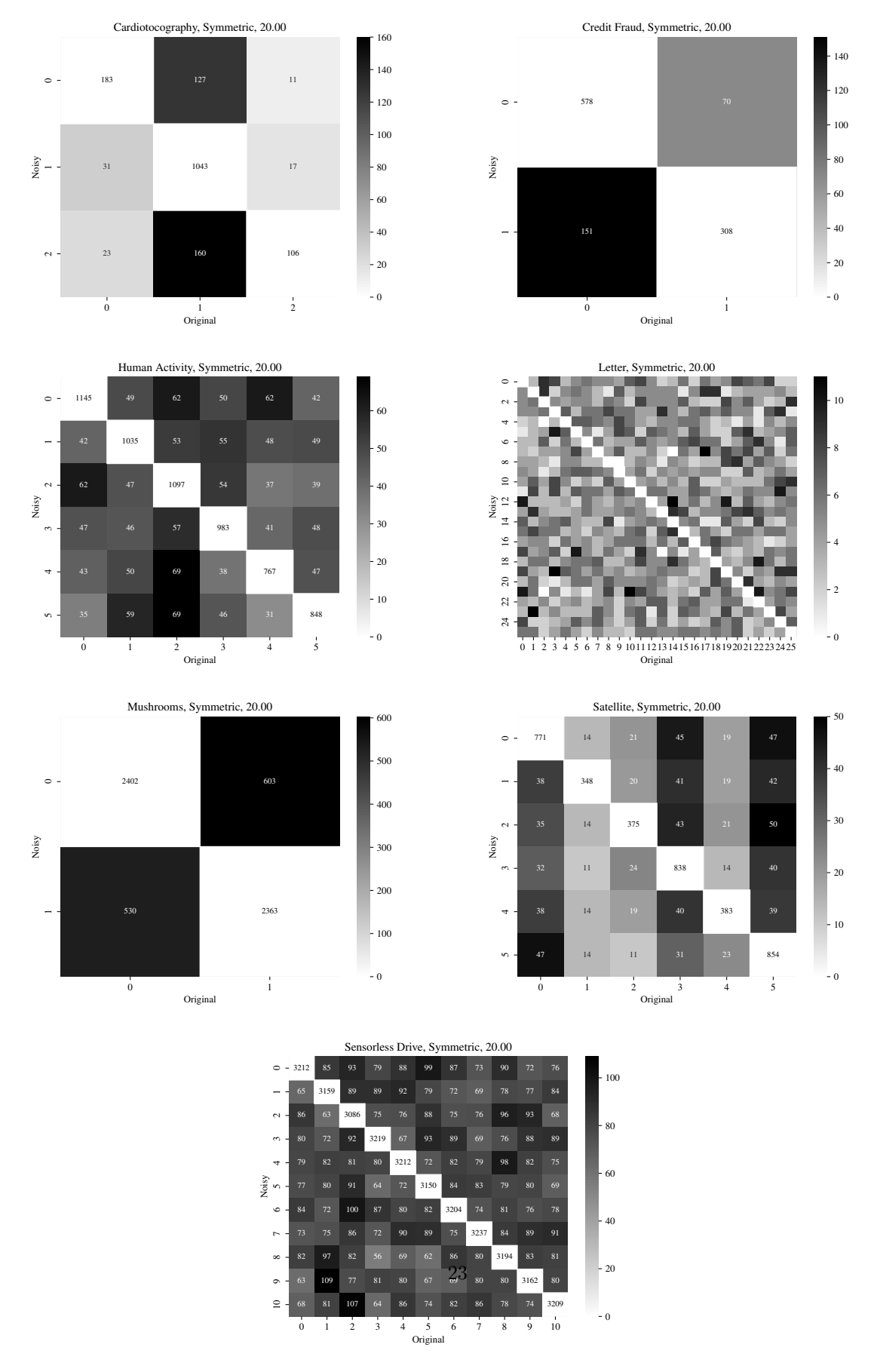


Figure A.9: Contingency tables for synthetic noise tabular datasets.

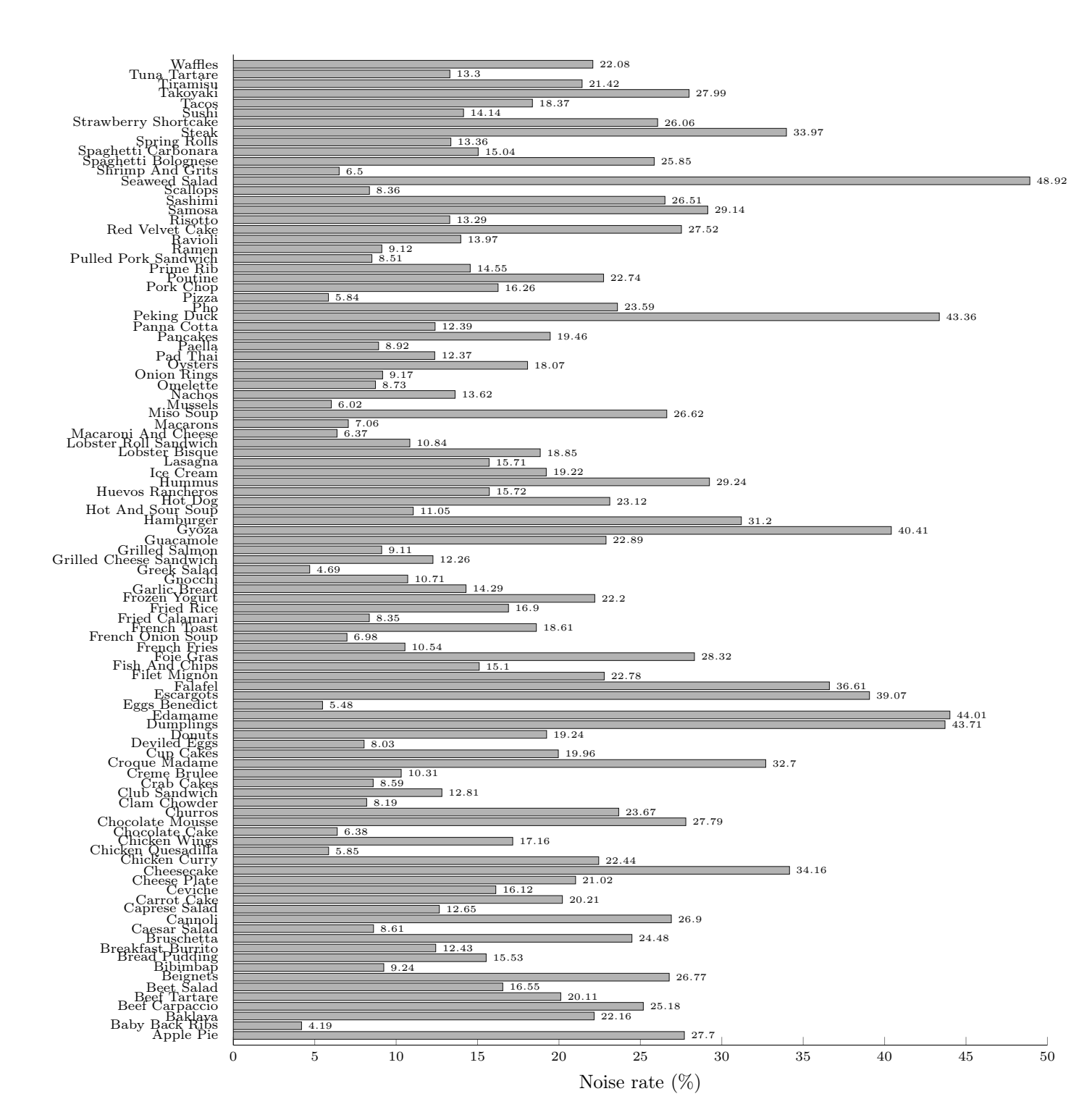


Figure A.10: Noise rate per noisy class, $P(y \neq \tilde{y}|\tilde{y})$, for the Food-101N dataset.

				Batch Size Optimizer	Optimizer	Epochs	Epochs Scheduler
Dataset	Noise Type	Noise Type Noise Rate Model	Model		•	•	
CIFAR-10	Aggregate	9.01%	9-Layer CNN	64	$Adam(lr=3e-05, weight_decay=0.03)$	100	$0.50,80 \; / \; 1.0,0.1,0.01$
	Worse	40.21%	9-Layer CNN	64	Adam(lr=0.0003, weight_decay=0.0002)	35	$0,25 \; / \; 1.0,0.1$
	Pairflip	20.00%	9-Layer CNN	128	Adam(lr=0.001, weight_decay=0.0001)	63	$0,50 \ / \ 1.0,0.1$
	Symmetric	20.00%	9-Layer CNN	64	Adam(lr=5e-05, weight_decay=0.02)	63	$0,50 \ / \ 1.0,0.1$
		20.00%	9-Layer CNN	32	Adam(lr=0.0001, weight_decay=0.001)	09	$0,50 \ / \ 1.0,0.1$
CIFAR-100	Pairflip	20.00%	9-Layer CNN	64	Adam(lr=5e-05, weight_decay=0.01)	101	$0.50,75 \ / \ 1.0,0.1,0.01$
	Symmetric	20.00%	9-Layer CNN	64	Adam(lr=0.0001, weight_decay=0.01)	92	$0.50,75 \ / \ 1.0,0.1,0.01$
		20.00%	9-Layer CNN	64	$Adam(lr=5e-05, weight_decay=0.005)$	62	$0.50 \ / \ 1.0,0.1$
Cardioto-							
$\operatorname{cography}$	Symmetric	20.00%	MLP	1024	$Adam(lr=0.01, weight_decay=0.0)$	206	
Clothing 1M	Real	38.26%	ResNet-18	64	Adam(lr=0.001, weight_decay=5e-05)	189*	$0,100 \ / \ 1.0,0.01$
Credit Frand	Symmetric 90 00%	200.00	MLP	1094	Adam (11-0 001 maight docar-0 001)	740	
riana	Symmetric	20.0070	INITI	1071	radin(m-0.001, weight accay -0.001)	071	
Food-101N	Real	18.51%	ResNet-34	64	SGD(lr=0.04, weight_decay=0.0005, momentum=0.0)	248*	$0,200 \mid 1.0,0.1$
Human Activity	Symmetric	20.00%	MI,P	1024	Adam($lr=0.001$. weight $decav=0.001$)	262	
Letter	Symmetric	20.00%	MLP	1024	Adam(lr=0.001, weight decay=0.0)	785	
Mushroom	Symmetric	20.00%	MLP	1024	$Adam(lr=0.0001, weight_decay=0.001)$	344	
Satellite	Symmetric	20.00%	MLP	1024	Adam(lr=0.001, weight_decay=0.001)	722	
Sensorless Drive	Symmetric	20.00%	MLP	1024	Adam(lr=0.001, weight_decay=0.001)	797	

Table B.12: Hyperparameters used for training. The Scheduler column lists the parameters of a step scheduler that adjusts the learning rate relative to the initial learning rate. It shows two lists of numbers separated by a forward slash where the first refers to the epochs and the second refers to the values that the initial learning rate should be multiplied by. The epoch values for Clothing1M and Food-101N are mini-epochs instead, where a mini-epoch is 1/20th and 1/10th of an epoch, respectively.

Appendix C. Classification Performances

Dataset	Noise Type	Noise Rate (%)	Model Architecture	Accuracy (%)
CIFAR-10	Pairflip	20.00	9-Layer CNN	90.02
	Symmetric	20.00	9-Layer CNN	89.21
	Symmetric	50.00	9-Layer CNN	81.77
CIFAR-10N	Aggregate	9.01	9-Layer CNN	90.33
	Worse	40.21	9-Layer CNN	81.57
CIFAR-100	Pairflip	20.00	9-Layer CNN	68.78
	Symmetric	20.00	9-Layer CNN	63.72
	Symmetric	50.00	9-Layer CNN	56.07
Clothing1M	Real	38.26	ResNet-18	68.73
Food-101N	Real	18.51	ResNet-34	77.92
Cardiotocography	Symmetric	20.00	MLP	78.59
Credit Fraud	Symmetric	20.00	MLP	94.58
Human Activity	Symmetric	20.00	MLP	76.62
Letter	Symmetric	20.00	MLP	90.58
Mushrooms	Symmetric	20.00	MLP	99.19
Satellite	Symmetric	20.00	MLP	88.25
Sensorless Drive	Symmetric	20.00	MLP	98.55

Table C.13: Classification performance achieved on each setting as measured on the clean test set.

Appendix D. Detection Hyperparameters

Table D.14 provides the hyperparameters for each method that achieved best performance on a tuning set of varying size. The table on the left provides the parameters for vision datasets, and the table on the right for tabular datasets.

		Model				9-Layer CNN	CNN				ResNet-18	ResNet-34
Noise type Aggregate Worse Pairflip Symmetric Pairflip Fraction 0.01% 40.21% 20.00% 50.00% 50.00% 20.10 20.10 20.10 2		Dataset		G	FAR-10				TFAR-100		Clothing1M	Food-101N
Noise rate 9.01% 40.21% 20.00% 20.00% 50.00% 20.00% Fraction 100 35 63 63 63 50.00% 20.00% 1% 44 57 61 56 53 184 5% 64 32 56 56 58 184 10% 64 46 56 61 55 184 10% 64 46 56 61 58 184 10% 64 46 56 61 55 184 10% 64 46 56 61 55 184 10% 64 46 56 61 184 184 5% 89-134 29-69 56-114 17-122 48-55 17-192 10% 73-134 26-66 51-73 25-104 29-72 180-196 0% 0-100 0-35 0-63 0-63 0-60 0-101 <th></th> <th>Noise type</th> <th>Aggregate</th> <th>Worse</th> <th>Pairflip</th> <th>Symn</th> <th>netric</th> <th>Pairflip</th> <th>Symn</th> <th>Symmetric</th> <th>Real</th> <th>Real</th>		Noise type	Aggregate	Worse	Pairflip	Symn	netric	Pairflip	Symn	Symmetric	Real	Real
Fraction 35 63 63 60 101 1% 44 57 61 56 53 184 5% 64 32 56 56 58 184 10% 64 46 56 61 55 184 10% 64 46 56 61 55 184 10% 64 46 56 61 55 184 10% 0-100 0-35 0-63 0-63 0-60 0-101 1% 29-139 30-63 0-63 0-60 0-101 18-188 1% 29-134 29-69 56-114 17-122 48-55 172-192 10% 7-3-134 26-66 51-73 25-10 29-73 180-196 0% 0-100 0-35 0-63 0-63 0-63 0-63 0-101 1% 1% 36-81 17-122 48-59 17-94 15-180		Noise rate	9.01%	40.21%	20.00%	20.00%	20.00%	20.00%	20.00%	20.00%	38.26%	18.51%
0% 100 35 63 60 101 1% 44 57 61 56 53 184 5% 64 32 56 56 58 184 10% 64 46 56 61 55 184 10% 64 46 56 61 55 184 10% 24-129 30-67 63 0-60 0-101 1% 24-129 30-67 53-89 30-68 0-60 184-188 1% 89-134 29-69 56-114 17-122 48-55 172-192 10% 73-134 26-66 51-73 25-104 29-72 180-196 0% 0-100 0-35 0-63 0-60 0-101 0% 0-100 0-35 36-32 2-114 17-94 151-180 1% 1% 40-121 21-38 35-73 31-68 164-196 10% 64,3,2)	Method	Fraction										
1% 44 57 61 56 53 184 5% 64 32 56 56 58 184 10% 64 46 56 56 58 184 0% 040 0-35 0-63 0-63 0-60 0-101 1% 24-129 30-67 53-89 30-68 0-60 184-188 1% 89-134 29-69 56-114 17-122 48-55 172-192 10% 773-134 26-66 51-73 25-104 29-72 180-196 0% 0-100 0-35 0-63 0-63 0-60 0-101 0% 0-100 0-35 0-63 0-63 0-60 0-101 1% 1% 36-81 15-32 38-63 2-114 17-94 151-180 1% 2 40-121 21-38 35-76 96-125 21-92 164-196 1% 40-121 14-39 45-73		%0	100	35	63	63	09	101	92	62	189	248
5% 64 32 56 56 58 184 10% 64 46 56 61 55 184 0% 0-100 0-35 0-63 0-63 0-60 0-101 1% 24-129 30-67 53-89 30-68 0-60 184-188 5% 89-134 29-69 56-114 17-122 48-55 172-192 10% 73-134 26-66 51-73 25-10 29-73 180-196 0% 0-100 0-35 0-63 0-63 0-60 0-101 0% 0-100 0-35 0-63 0-63 0-60 0-101 1% 1% 36-81 15-32 38-63 2-114 17-94 151-180 10% 40-121 21-38 35-76 96-125 21-92 164-196 10% 52-121 14-39 45-73 35-73 44, 3, 2) 4, 3, 2) 4, 3, 2) 4, 3, 2) 4, 3, 2) 4, 3, 2)) T/ (I/) T/	1%	44	22	61	26	53	184	74	52	278	213
10% 64 46 56 61 55 184 0% 0-100 0-35 0-63 0-63 0-60 0-101 1% 24-129 30-67 53-89 30-68 0-60 184-188 5% 89-134 29-69 56-114 17-122 48-55 172-192 10% 73-134 26-66 51-73 25-104 29-72 180-196 0% 0-100 0-35 0-63 0-63 0-60 0-101 1% 36-81 15-32 38-63 2-114 17-94 151-180 1% 40-121 21-38 35-76 96-125 21-92 164-196 10% 52-121 14-39 45-73 35-73 31-68 118-184 0% (4, 3, 2) (4, 3, 2) (4, 3, 2) (4, 3, 2) (4, 3, 2) (4, 3, 2) (4, 3, 2) (4, 3, 2) (4, 3, 2) (4, 3, 2) (4, 3, 2) (4, 3, 2) (4, 3, 2) (4, 3, 2) (4, 3, 2) (4, 3,	Last - CE/JS	2%	64	32	56	26	28	184	126	22	324	244
0% 0-100 0-35 0-63 0-63 0-60 0-101 1% 24-129 30-67 53-89 30-68 0-60 184-188 89-134 29-69 56-114 17-122 48-55 172-192 8 10% 73-134 26-66 51-73 25-104 29-72 180-196 70% 0-100 0-35 0-63 0-63 0-60 0-101 25% 40-121 21-32 38-63 2-114 17-94 151-180 10% 55% 40-121 21-38 35-76 96-125 21-92 164-196 10% 55% (4, 3, 2) (4, 3, 2) (4, 3, 2) (4, 3, 2) (4, 3, 2) (4, 3, 2) (4, 3, 2) (4, 3, 2) (4, 3, 2) (4, 3, 2) (4, 3, 2) (4, 3, 2) (4, 3, 2) (4, 3, 2) (4, 3, 2) (4, 3, 2) (4, 3, 2) (5, 2, 1) (8, 2, 1) (8, 2, 1) (8, 2, 1) (8, 2, 1) (8, 2, 2)		10%	64	46	56	61	55	184	74	22	324	244
$ \begin{array}{cccccccccccccccccccccccccccccccccccc$		%0	0-100	0-35	0-63	0-63	09-0	0-101	0-92	0-62	0 - 189	0-248
$ \begin{array}{cccccccccccccccccccccccccccccccccccc$	TO	1%	24-129	30-67	53-89	30-68	09-0	184-188	82-89	40-85	278-278	203-254
$ \begin{array}{cccccccccccccccccccccccccccccccccccc$	Mean - CE	5%	89-134	29-69	56 - 114	17-122	48-55	172 - 192	85-141	47-57	332-371	193-305
$ \begin{array}{cccccccccccccccccccccccccccccccccccc$		10%	73-134	56-66	51-73	25 - 104	29-72	180 - 196	70-145	35-65	278-379	203-264
$ \begin{array}{cccccccccccccccccccccccccccccccccccc$		%0	0-100	0-35	0-63	0-63	09-0	0-101	0-92	0-62	0 - 189	0-248
LAM 5% 40-121 21-38 35-76 96-125 21-92 164-196 10% 52-121 14-39 45-73 35-73 31-68 118-184 0% (4, 3, 2) (4, 3, 2) (4, 3, 2) (4, 3, 2) (4, 3, 2) (4, 3, 2) (4, 3, 2) (4, 3, 2) (4, 3, 2) (5, 3, 2) (6,	Man Ducke IM	1%	36-81	15-32	38-63	2-114	17-94	151 - 180	59 - 70	70-80	0-270	203-244
10% 52-121 14-39 45-73 35-73 31-68 118-184 0% (4, 3, 2) (4, 3, 2) (4, 3, 2) (4, 3, 2) (4, 3, 2) (4, 3, 2) (4, 3, 2) (4, 3, 2) (4, 3, 2) (5, 4, 3, 2) (6, 3,	Mean Froda - LM	2%	40 - 121	21-38	35-76	96 - 125	21-92	164 - 196	3-145	37-70	0-239	213-264
0% (4, 3, 2) (4, 3, 2) (4, 3, 2) (4, 3, 2) (7, 3, 2) (8, 3, 2) (1, 3, 2) (1, 3, 2) (1, 3, 2, 1) (1, 3, 2, 1) (1, 3, 2, 3, 3, 3, 3, 3, 3, 3, 3, 3, 3, 3, 3, 3,		10%	52 - 121	14-39	45-73	35-73	31-68	118-184	44-97	40-70	23-301	203-244
1% (4,4,1) (8,4,3) (8,2,1) (5% (8,2,1) (8,2,1) (7,8,4,3) (7,8,4,3) (7,8,		%0	(4, 3, 2)	(4, 3, 2)	(4, 3, 2)	(4, 3, 2)	(4, 3, 2)	(4, 3, 2)	(4, 3, 2)	(4, 3, 2)	(4, 3, 2)	(4, 3, 2)
	TOTE OF	1%	(4, 4, 1)	(8, 4, 3)	(8, 2, 1)	(8, 2, 1)	(2, 2, 1)	(8, 2, 1)	(8, 2, 1)	(2, 2, 1)	(4, 4, 3)	(8, 2, 1)
	20 - THE	2%	(8, 2, 1)	(8, 4, 3)	(8, 2, 1)	(8, 2, 1)	(8, 2, 1)	(8, 2, 1)	(8, 8, 3)	(8, 2, 1)	(4, 4, 3)	(8, 2, 1)
$10\% \qquad \qquad (8,2,1) \qquad (8,4,3) \qquad (8,2,1) \qquad (8,2,1) \qquad (8,2,1) \qquad (8,8,3)$		10%	(8, 2, 1)	(8, 4, 3)	(8, 2, 1)	(8, 2, 1)	(8, 2, 1)	(8, 2, 1)	(8, 8, 3)	(8, 2, 1)	(4, 4, 3)	(4, 2, 1)

	Model				MLP			
	Dataset	Cardioto- cography	Credit Fraud	Human Activity	Letter	Mushroom	Satellite	Sensorless Drive
	Noise type	Symmetric	Symmetric	Symmetric	Symmetric	Symmetric	Symmetric	Symmetric
	Noise rate	20.00%	20.00%	20.00%	20.00%	20.00%	20.00%	20.00%
Method	Fraction							
	%0	206	749	797	785	344	722	797
01/40/7	1%	32	30	65	96	48	28	357
Last - CE/JS	2%	32	336	130	160	65	412	1560
	10%	32	427	162	160	114	971	1560
	%0	0-206	0-749	0-797	0-785	0-344	0-722	0-797
Moon	1%	0-32	0-61	0-65	0-544	0-32	0-58	0 - 130
Mean - OE	2%	16-65	0-274	0 - 195	0-288	0-114	412-412	0-552
	10%	0-48	0-336	65-325	64-416	0-179	971-971	0-552
	%0	0-206	0-749	0-797	0-785	0-344	0-722	0-797
Moon Ducke IM	1%	16-32	0-61	0-65	809-0	0-32	971-971	0 - 162
Mean Froba - LM	2%	16-48	0-305	0 - 195	0-224	26-0	0 - 117	0-357
	10%	0-65	0 - 336	97-260	0-288	0 - 179	0-58	32-357
	%0	(4, 5, 3, 2)	(4, 5, 3, 2)	(4, 5, 3, 2)	(4, 5, 3, 2)	(4, 5, 3, 2)	(4, 5, 3, 2)	(4, 5, 3, 2)
GTD I GTD	1%	(2, 5, 2, 1)	(4, 5, 2, 1)	(2, 5, 2, 1)	(8, 5, 2, 1)	(8, 5, 2, 1)	(2, 5, 2, 1)	(2, 5, 2, 1)
OINT - OE	2%	(4, 5, 4, 3)	(2, 5, 2, 1)	(4, 5, 2, 1)	(4, 5, 2, 1)	(8, 5, 4, 1)	(2, 5, 2, 1)	(4, 5, 2, 1)
	10%	(4, 5, 2, 1)	(2, 5, 2, 1)	(8, 5, 2, 1)	(4, 5, 2, 1)	(8, 5, 4, 1)	(2, 5, 2, 1)	(8, 5, 2, 1)

Table D.14: Optimized hyperparameters for each detection method on varying fractions of labeled samples. For the Last method the value indicates the single epoch used for calculating the scores. For Mean - CE and Mean Proba - LM, it indicates the range of epochs used for calculating scores. For CTRL - CE it provides the parameters for the number of windows, the total number of clusters used in K-means for each window and the number of selected clusters, respectively.

References

- [1] C. Northcutt, L. Jiang, I. Chuang, Confident learning: Estimating uncertainty in dataset labels, Journal of Artificial Intelligence Research 70 (2021) 1373–1411.
- [2] C. G. Northcutt, A. Athalye, J. Mueller, Pervasive label errors in test sets destabilize machine learning benchmarks, Tech. Rep. arXiv:2103.14749, arXiv, type: article (2021). arXiv:2103.14749[cs,stat]. URL http://arxiv.org/abs/2103.14749
- [3] B. Frenay, M. Verleysen, Classification in the presence of label noise: A survey, IEEE Transactions on Neural Networks and Learning Systems 25 (5) (2014) 845–869. doi:10.1109/TNNLS.2013.2292894.
- [4] C. Zhang, S. Bengio, M. Hardt, B. Recht, O. Vinyals, Understanding deep learning (still) requires rethinking generalization, Commun. ACM 64 (3) (2021) 107–115. doi:10.1145/3446776.
- [5] H. Song, M. Kim, D. Park, Y. Shin, J.-G. Lee, Learning from noisy labels with deep neural networks: A survey, IEEE Transactions on Neural Networks and Learning Systems 34 (11) (2023) 8135–8153. doi:10.1109/TNNLS.2022.3152527.
- [6] J. Huang, L. Qu, R. Jia, B. Zhao, O2u-net: A simple noisy label detection approach for deep neural networks, in: 2019 IEEE/CVF International Conference on Computer Vision (ICCV), 2019, pp. 3325– 3333.
- [7] B. Han, Q. Yao, X. Yu, G. Niu, M. Xu, W. Hu, I. Tsang, M. Sugiyama, Co-teaching: Robust training of deep neural networks with extremely noisy labels, in: S. Bengio, H. Wallach, H. Larochelle, K. Grauman, N. Cesa-Bianchi, R. Garnett (Eds.), Advances in Neural Information Processing Systems, Vol. 31, Curran Associates, Inc., 2018.
- [8] J. Li, R. Socher, S. C. H. Hoi, Dividemix: Learning with noisy labels as semi-supervised learning, in: Proceedings of the International Conference on Learning Representations (ICLR), 2020, pp. 1–14.
- [9] N. Karim, M. N. Rizve, N. Rahnavard, A. Mian, M. Shah, Unicon: Combating label noise through uniform selection and contrastive learning, in: 2022 IEEE/CVF Conference on Computer Vision and Pattern Recognition (CVPR), 2022, pp. 9666–9676.
- [10] E. Arazo, D. Ortego, P. Albert, N. O'Connor, K. Mcguinness, Unsupervised label noise modeling and loss correction, in: K. Chaudhuri, R. Salakhutdinov (Eds.), Proceedings of the 36th International Conference on Machine Learning, Vol. 97 of Proceedings of Machine Learning Research, PMLR, 2019, pp. 312–321.
- [11] C. Tan, J. Xia, L. Wu, S. Z. Li, Co-learning: Learning from noisy labels with self-supervision, in: Proceedings of the 29th ACM International Conference on Multimedia, MM '21, Association for Computing Machinery, New York, NY, USA, 2021, p. 1405–1413. doi:10.1145/3474085.3475622.
- [12] D. Chen, Z. Yu, S. R. Bowman, Clean or annotate: How to spend a limited data collection budget, in: C. Cherry, A. Fan, G. Foster, G. R. Haffari, S. Khadivi, N. V. Peng, X. Ren, E. Shareghi, S. Swayamdipta (Eds.), Proceedings of the Third Workshop on Deep Learning for Low-Resource Natural Language Processing, Association for Computational Linguistics, Hybrid, 2022, pp. 152–168. doi:10.18653/v1/ 2022.deeplo-1.17.
- [13] G. Zhao, G. Li, Y. Qin, F. Liu, Y. Yu, Centrality and consistency: Two-stage clean samples identification for learning with instance-dependent noisy labels, in: S. Avidan, G. Brostow, M. Cissé, G. M. Farinella, T. Hassner (Eds.), Computer Vision ECCV 2022, Springer Nature Switzerland, Cham, 2022, pp. 21–37.
- [14] C. Yue, N. K. Jha, Ctrl: Clustering training losses for label error detection, IEEE Transactions on Artificial Intelligence 5 (8) (2024) 4121–4135.

- [15] G. Pleiss, T. Zhang, E. Elenberg, K. Q. Weinberger, Identifying mislabeled data using the area under the margin ranking, in: H. Larochelle, M. Ranzato, R. Hadsell, M. Balcan, H. Lin (Eds.), Advances in Neural Information Processing Systems, Vol. 33, Curran Associates, Inc., 2020, pp. 17044–17056.
- [16] J. Chen, A. Martel, Cross-validation is all you need: A statistical approach to label noise estimation (2023). arXiv:2306.13990[cs], doi:10.48550/arXiv.2306.13990. URL http://arxiv.org/abs/2306.13990
- [17] Z. Zhu, Z. Dong, Y. Liu, Detecting corrupted labels without training a model to predict (2022). arXiv: 2110.06283[cs], doi:10.48550/arXiv.2110.06283.
 URL http://arxiv.org/abs/2110.06283
- [18] D. Arpit, S. Jastrzębski, N. Ballas, D. Krueger, E. Bengio, M. S. Kanwal, T. Maharaj, A. Fischer, A. Courville, Y. Bengio, S. Lacoste-Julien, A closer look at memorization in deep networks, in: D. Precup, Y. W. Teh (Eds.), Proceedings of the 34th International Conference on Machine Learning, Vol. 70 of Proceedings of Machine Learning Research, PMLR, 2017, pp. 233–242.
- [19] G. Huang, Y. Li, G. Pleiss, Z. Liu, J. E. Hopcroft, K. Q. Weinberger, Snapshot ensembles: Train 1, get m for free (2017). arXiv:1704.00109[cs], doi:10.48550/arXiv.1704.00109. URL http://arxiv.org/abs/1704.00109
- [20] S. Swayamdipta, R. Schwartz, N. Lourie, Y. Wang, H. Hajishirzi, N. A. Smith, Y. Choi, Dataset cartography: Mapping and diagnosing datasets with training dynamics, in: Proceedings of the 2020 Conference on Empirical Methods in Natural Language Processing (EMNLP), Association for Computational Linguistics, 2020, pp. 9275-9293. doi:10.18653/v1/2020.emnlp-main.746. URL https://www.aclweb.org/anthology/2020.emnlp-main.746
- [21] P. Chen, B. B. Liao, G. Chen, S. Zhang, Understanding and utilizing deep neural networks trained with noisy labels, in: K. Chaudhuri, R. Salakhutdinov (Eds.), Proceedings of the 36th International Conference on Machine Learning, Vol. 97 of Proceedings of Machine Learning Research, PMLR, 2019, pp. 1062–1070.